

COMPUTATION OF CONFORMAL INVARIANTS

MOHAMED M S NASSER AND MATTI VUORINEN

ABSTRACT. We study numerical computation of conformal invariants of domains in the complex plane. In particular, we provide an algorithm for computing the conformal capacity of a condenser. The algorithm applies for wide kind of geometries: domains are assumed to have smooth or piecewise smooth boundaries. The method we use is based on the boundary integral equation method developed and implemented in [N3]. A characteristic feature of this method is that, with small changes in the code, a wide spectrum of problems can be treated and we include code snippets within the text to indicate implementation details. We compare the performance and accuracy to previous results in the cases when numerical data is available and also in the case of several model problems where exact results are available.

1. INTRODUCTION

During the past fifty years conformal invariants have become crucial tools for complex analysis. Most important of these invariants are the harmonic measure, the conformal capacity, the extremal length, and the hyperbolic distance [Ah, GM, KL, ST]. But this is not all: the generalized capacity, the transfinite diameter, the reduced extremal length, the hyperbolic area, and the modulus metric [Du, Ki, Va, V1, V2] are some additional examples. Some of the many applications of these tools are discussed in the articles of the handbook [Ku]. In view of the plenitude of these applications, it is surprising that these invariants can be expressed explicitly only in very few special cases. Sometimes rudimentary upper or lower bounds for conformal invariants in terms of less involved comparison functions can provide important steps in proofs.

At the same time it seems that the full power of conformal invariance remains unused. One reason for this is that the analytic expressions for conformal invariants are usually too complicated for pen and paper calculations and the existing computational methods are scattered throughout the mathematical literature: the way from theory to practical experimentation is too long. On the other hand, the creators of the existing computational methods may not be aware of the scope of applicability of their methods in theoretical studies: the way from experiments to theory is also long. If the distance from theory to experiments could be made shorter, a theoretical researcher could easily experiment the dependence of a problem under perturbation of geometry and vice versa a computational scientist would find new types of benchmark problems and areas of application.

2010 *Mathematics Subject Classification.* 65E05, 30C85, 31A15.

Key words and phrases. Conformal capacity; hyperbolic capacity; elliptic capacity; boundary integral equations; numerical conformal mapping.

File: ccc20190813.tex, printed: 2019-8-14, 0.36

The above ideas as our guiding principles, we have written a series of papers of which this is the first one [KNV, NV]. As far as we know, our work is the first attempt to provide computational tools for a wide class of conformal invariants with the feature that modification of geometry is simple. The method we use was developed and implemented by the first author [N3] and we apply it to study several computational problems never studied before and we also compare its performance to several results in the literature. As test problems we use the computation of condenser capacity, a topic studied by the second author in several papers [HRV1, HRV2, HRV3].

A condenser is a pair (D, C) where D is an open set in \mathbb{R}^2 and $C \subset D$ is compact. In our study we assume that the topology is simple but still general enough for most applications: the sets ∂D and ∂C are connected sets, each set is a piecewise smooth Jordan curve.

The conformal capacity, or capacity for short, is defined by [Du]

$$(1.1) \quad \text{cap}(D, C) = \int_D |\nabla u|^2 dm$$

where $u : D \rightarrow \mathbb{R}$ is a harmonic function with $u(x) \geq 1$ for all $x \in C$ and $u(x) \rightarrow 0$ for $x \rightarrow \partial D$. The domain $G = D \setminus C$ is called the field of the condenser and the closed sets C and D^c are called the plates of the condenser. Then, the capacity $\text{cap}(D, C)$ may alternatively be written as $\text{cap}(G)$.

In literature, only very few formulas are given for the capacities of concrete condensers. Numerical methods are therefore needed to compute the value of (1.1). Our problem is reduced to the classical problem of solving numerically the Dirichlet boundary value problem for the Laplace equation. Moreover, by the Dirichlet principle [GM, pp. 447-456], the extremal function u_0 is harmonic and minimizes the integral [Ah], [GM, pp.441-456]:

$$(1.2) \quad \int_D |\nabla u_0|^2 dm = \inf \left\{ \int_D |\nabla u|^2 dm \right\}$$

where the infimum is taken over all $C_o(D)$ functions with the indicated Dirichlet boundary values. The capacity of condensers is invariant under conformal mappings, and hence domains with difficult geometry can be handled with the help of conformal mappings [AVV, DT, Du, PS, SL, Va, V2]. See also [BBG, DEK, ET].

Before proceeding to the contents of our work a few general remarks about the literature we know about may be in order. Because of the wide scope of conformal invariants, relatively few cases exist where “the right answer” is known. In such cases, the computational performance may be analysed by observing convergence features of the results under successive refinements of the numerical model, and error estimates maybe based on general theory. In those relatively few cases we have found in the literature where the analytic formula is known, the true error estimate may be given. Sometimes a high accuracy can be achieved, say 12 decimal places, but the dilemma is that if the geometry of the problem is smoothly changed a bit, the method might not be applicable at all.

Section 2 summarizes our computational workhorse, the boundary integral method geared for the capacity computation of ring domains, which will be applied in several later sections, sometimes together with auxiliary procedures. In Sections 3 and 5 we consider

ring domains for which the exact value of capacity is known and investigate the performance of our method. Sections 4, 6, and 7 deal with condensers whose one or two complementary components are slits—these are well-known examples computationally challenging problems and we use here auxiliary conformal mapping to overcome computational difficulties. Section 8 deals with the case when both complementary components of a ring domain are thin rectangles. In Section 9, we consider the numerical computation of the hyperbolic capacity and the elliptic capacity of compact and closed sets. The final Section 10 gives some concluding remarks and information about the access to our MATLAB software.

CONTENTS

1. Introduction	1
2. Conformal mapping onto annulus	3
3. Rings with piecewise smooth boundaries	9
4. Complement of two slits	14
5. Rings with a segment as a boundary component	17
6. The upper half-plane with a slit	26
7. A strip with a slit	29
8. Domains exterior to thin rectangles	34
9. The hyperbolic capacity and the elliptic capacity	39
10. Concluding Remarks	45
References	45

2. CONFORMAL MAPPING ONTO ANNULUS

2.1. Ring domains. A domain G in the extended complex plane $\overline{\mathbb{C}} = \mathbb{C} \cup \{\infty\}$, whose complement $\overline{\mathbb{C}} \setminus G$ has two components, is called a ring domain or, briefly, a ring. It is a classical fact that a ring can be mapped by a conformal map onto an annulus $\{z : q < |z| < 1\}$, $q \in (0, 1)$. A ring R is the simplest example of a condenser and its capacity is given by [Du], [GM, p. 132-133]

$$\text{cap}(R) = \frac{2\pi}{\log(1/q)}.$$

The number $\log(1/q)$ is called the modulus of the ring, i.e.,

$$(2.2) \quad M(R) = \log(1/q) = \frac{2\pi}{\text{cap}(R)}.$$

Because of the conformal invariance of the capacity, this definition is independent of the conformal map. For the computation of the capacity we will often use an auxiliary conformal mapping to avoid computational singularities.

In this section we describe the method of our numerical work, based on the solution of the boundary integral equation with the generalized Neumann kernel [N3, WN]. The integral equation has been applied to calculate conformal mappings onto several canonical

domains [N1, N4, NF]. We review the application of the integral equation to compute the conformal mapping from doubly connected domains onto an annulus $\{z : q < |z| < 1\}$, $q \in (0, 1)$, and present the MATLAB implementation of the method. In later sections we will apply this method for capacity computation of several condensers, in particular we will consider several types of rings with a simple geometric structure.

2.3. The generalized Neumann kernel. Let G be a bounded or an unbounded doubly connected domain bordered by

$$\Gamma = \partial G = \Gamma_1 \cup \Gamma_2$$

where each of the boundary components Γ_1 and Γ_2 is a closed smooth Jordan curve. We choose the orientation of boundary Γ such that when we proceed along Γ , the domain G is always on its left. If G is bounded, then Γ_1 is the external boundary and Γ_2 is contained in the bounded domain whose boundary is $\overline{\Gamma_1}$. The complement $\overline{\mathbb{C}} \setminus \overline{G}$ of the domain G with respect to the extended complex plane $\overline{\mathbb{C}}$ consists of two simply connected domains G_1 on the right of Γ_1 and G_2 on the right of Γ_2 . The domain G_2 is bounded and the domain G_1 is unbounded with $\infty \in G_1$. Further, we assume α is an auxiliary given point in the domain G and z_2 is an auxiliary given point in the simply connected domain G_2 . When G is unbounded, then $\infty \in G$ and the two domains G_1 and G_2 are bounded. We assume that z_1 and z_2 are auxiliary given points in the simply connected domains G_1 and G_2 , respectively. See Figure 1.

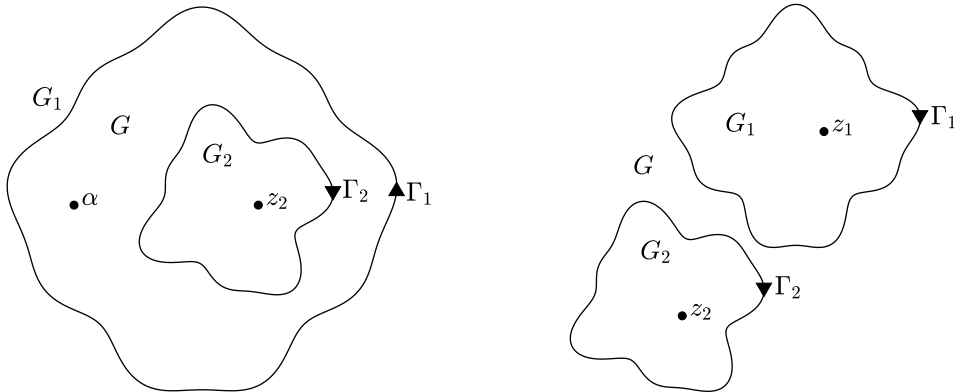


FIGURE 1. An example of bounded (left) and unbounded (right) doubly connected domain G .

We parametrize each boundary component Γ_j by a 2π -periodic complex function $\eta_j(t)$, $t \in J_j := [0, 2\pi]$, $j = 1, 2$. We assume that each of these functions $\eta_j(t)$ is twice continuously differentiable with $\eta_j'(t) \neq 0$ (the presented method can be applied also if the curve Γ_j have a finite number of corner points but no cusps [NMZ]). Then we define the total parameter domain J as the disjoint union of the two intervals $J_1 = [0, 2\pi]$ and $J_2 = [0, 2\pi]$, i.e., $J = J_1 \sqcup J_2 = \cup_{j=1}^2 \{(t, j) : t \in J_j\}$. The elements of the total parameter domain J are ordered pairs (t, j) where t is a real number, $0 \leq t \leq 2\pi$, and the index j is an integer indicates that the interval J_j containing t [N3]. Hence, the boundary Γ can be parametrized

by

$$(2.4) \quad \eta(t, j) = \eta_j(t), \quad t \in J_j, \quad j = 1, 2.$$

For a given t , the index k such that $t \in J_k$ will be always clear from the context, see e.g., [N1, N3, NF, NG, WN]. So the pair (t, k) in the left-hand side of (2.4) will be replaced by t and a parametrization of the whole boundary Γ can be defined on J by

$$(2.5) \quad \eta(t) = \begin{cases} \eta_1(t), & t \in J_1, \\ \eta_2(t), & t \in J_2. \end{cases}$$

We denote by H to the space of all functions of the form

$$\rho(t) = \begin{cases} \rho_1(t), & t \in J_1, \\ \rho_2(t), & t \in J_2, \end{cases}$$

where $\rho_1(t)$ and $\rho_2(t)$ are 2π -periodic Hölder continuous real functions on J_1 and J_2 , respectively.

Let A be the complex function [N3]

$$(2.6) \quad A(t) = \begin{cases} e^{i(\frac{\pi}{2}-\theta(t))}(\eta(t) - \alpha), & \text{if } G \text{ is bounded,} \\ e^{i(\frac{\pi}{2}-\theta(t))}, & \text{if } G \text{ is unbounded,} \end{cases}$$

where θ is a real function with constant value on each interval J_j , i.e.,

$$\theta(t) = \theta_j \quad \text{for } t \in J_j$$

and θ_j is a real constant, $j = 1, 2$. The generalized Neumann kernel $N(s, t)$ is defined for $(s, t) \in J \times J$ by

$$(2.7) \quad N(s, t) := \frac{1}{\pi} \operatorname{Im} \left(\frac{A(s)}{A(t)} \frac{\dot{\eta}(t)}{\eta(t) - \eta(s)} \right).$$

The kernel $N(s, t)$ is continuous [WN]. Hence, the integral operator \mathbf{N} defined on by

$$\mathbf{N}\rho(s) := \int_J N(s, t)\rho(t)dt, \quad s \in J,$$

is compact. The integral equation with the generalized Neumann kernel involves also the following kernel

$$(2.8) \quad M(s, t) := \frac{1}{\pi} \operatorname{Re} \left(\frac{A(s)}{A(t)} \frac{\dot{\eta}(t)}{\eta(t) - \eta(s)} \right), \quad (s, t) \in J \times J,$$

which has a singularity of cotangent type [WN]. The integral operator \mathbf{M} defined on H by

$$\mathbf{M}\rho(s) := \int_J M(s, t)\rho(t)dt, \quad s \in J,$$

is singular, but is bounded on H [WN]. For more details, see [WN].

For the above function A defined by (2.6), the following integral equation

$$(2.9) \quad (\mathbf{I} - \mathbf{N})\rho = -\mathbf{M}\gamma$$

is uniquely solvable for any real function γ in H [N2]. Furthermore, if ρ is the unique solution of the boundary integral equation (2.9), then the real function h defined by

$$(2.10) \quad h = [\mathbf{M}\rho - (\mathbf{I} - \mathbf{N})\gamma]/2$$

is a piecewise constant function on the boundary Γ , i.e.,

$$h(t) = h_j \quad \text{for } \eta(t) \in \Gamma_j$$

where h_j is a real constant, $j = 1, 2$ [N2]. Moreover,

$$(2.11) \quad f(\eta(t)) = \frac{\gamma(t) + h(t) + i\rho(t)}{A(t)}, \quad \eta(t) \in \Gamma,$$

are boundary values of an analytic function f in the domain G with $f(\infty) = 0$ for unbounded G . For more details, see [N2, N3] and the references cited therein.

2.12. Numerical solution of the boundary integral equation. The MATLAB function `fbie` in [N3] provides us with a fast and efficient method for solving the boundary integral equation (2.9). The function `fbie` is based on discretizing the boundary integral equation (2.9) using the Nyström method with the trapezoidal rule [AKT, At, TW]. This discretization leads to a non-symmetric linear system. Then, the MATLAB function `gmres` is used to solve the linear system. The matrix-vector multiplication in the GMRES method is computed using the MATLAB function `zfmm2dpart` in the toolbox `FMMLIB2D` [GG]. The function `fbie` provides us also with approximations to the piecewise constant function h in (2.10). The computational cost for the overall method is $O(n \log n)$ operations where n (an even positive integer) is the number of nodes in each of the intervals J_1 and J_2 .

For the accuracy of the obtained numerical results, it is known that the order of the convergence of the Nyström method depends on the order of convergence of the used quadratic method [At]. The quadratic method used in the function `fbie` is the trapezoidal rule which gives surprisingly accurate numerical results for periodic functions [At, TW]. In view of (2.7) and (2.8), the smoothness of the two kernels $N(s, t)$ and $M(s, t)$ depends on the smoothness of the parametrization function $\eta(t)$. Similarly, in this paper, the function γ on the right-hand side of the integral equation (2.9) will be defined in terms of the parametrization $\eta(t)$. Hence, the smoothness of the function γ will depend also on the smoothness of the boundary Γ . Thus, the order of convergence of the trapezoidal rule depends on the smoothness of the boundary Γ of the domain G . For domain with smooth boundaries, we use the trapezoidal rule with equidistant nodes. Thus, for domains with C^∞ smooth boundaries, the integrand in the integral equation (2.9) will be C^∞ smooth and hence the rate of convergence of the numerical method is $O(e^{-cn})$ with a positive constant c (see [K2, p. 223]). If the boundary is C^{q+2} smooth ($q \geq 0$), then the function γ will be also C^{q+2} smooth and the rate of convergence of the numerical method is $O(1/n^q)$ [K1]. For domains with corners (excluding cusps), the trapezoidal rule with equidistant nodes yields only poor convergence and hence the trapezoidal rule with a graded mesh will be used [K1]. The graded mesh is obtained by substituting a new variable to remove the discontinuity in the derivatives of the solution $\rho(t)$ of the boundary integral equation (2.9) at the corner points [K1, LSN].

To use the MATLAB function `fbie`, the vectors `et`, `etp`, `A`, and `gam` that contain the discretizations of the functions $\eta(t)$, $\eta'(t)$, $A(t)$, and $\gamma(t)$, respectively, will be stored in MATLAB. Then we call the function

$$[\text{rho}, \text{h}] = \text{fbie}(\text{et}, \text{etp}, \text{A}, \text{gam}, \text{n}, \text{iprec}, \text{restart}, \text{gmrestol}, \text{maxit})$$

to compute the vectors `rho` and `h` which contain the discretizations of the solution of the integral equation $\rho(t)$ and the piecewise constant function $h(t)$, respectively. In the numerical experiments in this paper, we set the tolerances of the FMM and the GMRES to be 0.5×10^{-15} and 10^{-14} by choosing `iprec` = 5 and `gmrestol` = 10^{-14} , respectively. We use the GMRES without restart by choosing `restart` = []. The maximum number of iterations for GMRES is chosen to be `maxit` = 100.

Choosing the value of n depends on the geometry of the domain G . If the domain G has a simple geometry and smooth boundary, we can obtain accurate numerical results by choosing moderate values of n . If the domain G has a complex geometry such that its boundary has corners or its boundary components are close to each other, it is required to choose a sufficiently large value of n to obtain accurate results. For domains with corners, we choose n as a multiple of the number of corners.

Once the discretizations of the two functions $\rho(t)$ and $h(t)$ are computed, we can compute a discretization of the boundary values of the analytic function $f(z)$ through

$$\text{fet} = (\text{gam} + \text{h} + \text{i} * \text{rho}) ./ \text{A}.$$

Then approximations to the values of the function $f(z)$ for any vector of points \mathbf{z} in G can be obtained using the Cauchy integral formula. Numerically we carry out this computation by applying the MATLAB function `fcau` [N3] by calling

$$\text{fz} = \text{fcau}(\text{et}, \text{etp}, \text{fet}, \mathbf{z})$$

for bounded G and by calling

$$\text{fz} = \text{fcau}(\text{et}, \text{etp}, \text{fet}, \mathbf{z}, \text{n}, 0)$$

for unbounded G (here $0 = f(\infty)$).

For more details, we refer the reader to [N3].

The computations in this paper were performed in MATLAB R2017a on an ASUS Laptop with Intel(R) Core(TM) i7-8750H CPU @2.20GHz, 2208 Mhz, 6 Core(s), 12 Logical Processor(s), and 16GB RAM. The MATLAB `tic` `toc` commands were used to measure the computation times.

2.13. Computing the conformal mapping for bounded domains. If the domain G is bounded, then can compute the conformal mapping $w = \Phi(z)$ from G onto the annulus $\{w \in \mathbb{C} : q < |w| < 1\}$ with the normalization

$$\Phi(\alpha) > 0$$

as in the following theorem from [N1]. Here, α is an auxiliary given point in G .

Theorem 2.14. Let $\theta_1 = \theta_2 = \pi/2$, let the function A be defined by (2.6), and let the function γ be defined by

$$(2.15) \quad \gamma(t) = -\log \left| \frac{\eta(t) - z_2}{\alpha - z_2} \right|, \quad t \in J.$$

If ρ is the unique solution of the boundary integral equation (2.9) and the piecewise constant function h is given by (2.10), then the function f with the boundary values (2.11) is analytic in the domain G , the conformal mapping Φ is given by

$$(2.16) \quad \Phi(z) = e^{-h_1} \left(\frac{z - z_2}{\alpha - z_2} \right) e^{(z-\alpha)f(z)}, \quad z \in G \cup \Gamma,$$

and the modulus q is given by

$$(2.17) \quad q = e^{h_2 - h_1}.$$

2.18. Computing the conformal mapping for unbounded domains. For unbounded domain G , the following theorem from [N1] provides us with a method to compute the conformal mapping $w = \Phi(z)$ from G onto the annulus $\{w \in \mathbb{C} : q < |w| < 1\}$ with the normalization

$$\Phi(\infty) > 0.$$

Theorem 2.19. Let $\theta_1 = \theta_2 = \pi/2$, let the function A be defined by (2.6), and let the function γ be defined by

$$(2.20) \quad \gamma(t) = -\log \left| \frac{\eta(t) - z_2}{\eta(t) - z_1} \right|, \quad t \in J.$$

If ρ is the unique solution of the boundary integral equation (2.9) and the piecewise constant function h is given by (2.10), then the function f with the boundary values (2.11) is analytic in the domain G with $f(\infty) = 0$, the conformal mapping Φ is given by

$$(2.21) \quad \Phi(z) = e^{-h_1} \left(\frac{z - z_2}{z - z_1} \right) e^{f(z)}, \quad z \in G \cup \Gamma,$$

and the modulus q is given by

$$(2.22) \quad q = e^{h_2 - h_1}.$$

2.23. Computing the capacity of the doubly connected domain G . Since the capacity is invariant under conformal mapping, we shall compute the capacity of the above doubly connected domain G (for both cases, bounded and unbounded) by mapping G onto the annulus $R = \{w \in \mathbb{C} : q < |w| < 1\}$ using the method presented in the above two theorems. Then the capacity of G is the same as the capacity of the annulus R which is given by

$$(2.24) \quad \text{cap}(G) = \text{cap}(R) = \frac{2\pi}{\log(1/q)}.$$

The method presented in this section for computing the radius q of the inner circle of the annulus $R = \{w \in \mathbb{C} : q < |w| < 1\}$ and hence the capacity $\text{cap}(G)$ for both bounded

and unbounded doubly connected domains G can be implemented in MATLAB as in the following function.

```
function [q,cap] = annq (et,etp,n,zz,z2,type)
% This function computes the inner radius q for the conformal mapping
% w=Phi(z) from doubly connected domain G onto the annulus q<|w|<1 and
% the capacity of G, cap(G)=2pi/log(1/q), where:
% et, etp: the parametrization of the boundary of G and its derivative
% n: the number of discretization points
% zz: zz=alpha is a given point in $G$ for bounded G;
%      and zz=z1 is a given point in the interior of the curve that will be
%      mapped onto the unit circle for unbounded G
% z2: a given point interior to the curve that will be mapped onto the
% circle |w|=q for both cases of bounded and unbounded G.
% type='b' for bounded G; and type='u' for unbounded G
%
if type=='b'
    alpha = zz; A = et-alpha; gam = -log(abs((et-z2)./(alpha-z2)));
elseif type=='u'
    z1 = zz; A = ones(size(et)); gam = -log(abs((et-z2)./(et-z1)));
end
[~,h] = fbie(et,etp,A,gam,n,5,[],1e-14,200);
q = exp(mean(h(n+1:2*n))-mean(h(1:n)));
cap = 2*pi/log(1/q);
end
```

3. RINGS WITH PIECEWISE SMOOTH BOUNDARIES

In this section, we apply the method presented in Section 2 to compute the capacity of several doubly connected domains G with piecewise smooth boundaries. For the first two examples, the exact value of the capacity is known.

3.1. Two circles. In the first example, we consider the doubly connected domain in the exterior of the two circles $|z| = 1$ and $|z - a| = r$ where $r > 0$ and a is a real number with $a > 1 + r$.

Using a Möbius transform, the domain G can be mapped onto the annulus $\{w \in \mathbb{C} : q < |w| < 1\}$ where q is obtained by solving the following equation which follows from the invariance of the cross ratios under Möbius transformations [V2, (1.28)]

$$\frac{(1+q)^2}{q} = \frac{(1+a-r)(a+r-1)}{r}.$$

Hence, the exact value of conformal capacity is given by $\text{cap}(G) = 2\pi/\log(1/q)$.

We use the MATLAB function `annq` with $z_1 = 0$, $z_2 = a$ and $n = 2^{10}$ to compute approximate values for the capacity for several values of a and r . First, we fixed $r = 1$ and chose values of a between 2.01 and 6. The relative errors for the computed values

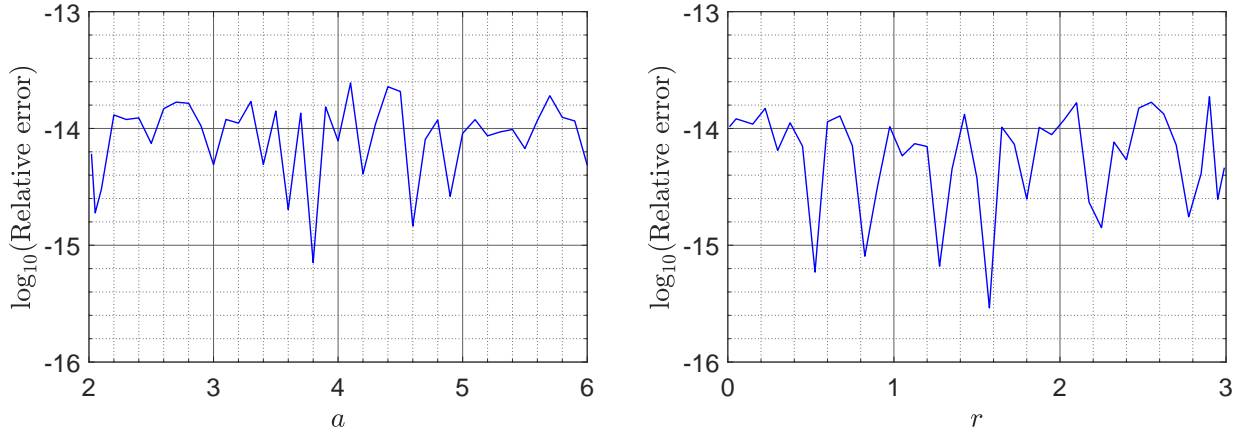


FIGURE 2. Results for the two circles domain: Relative errors of the computed conformal capacity for fixed $r = 1$ (left) and fixed $a = 4$ (right).

are presented in Figure 2(left). Then, we fixed $a = 4$ and chose values of r between 0.01 and 2.99. The relative errors for the computed values for this case are presented in Figure 2(right).

3.2. Two confocal ellipses. In this example, we consider the bounded doubly connected domain G in the interior of the ellipse

$$\eta_1(t) = \frac{1}{2} \left(r_1 e^{it} + \frac{1}{r_1} e^{-it} \right), \quad 0 \leq t \leq 2\pi,$$

and in the exterior of the ellipse

$$\eta_2(t) = \frac{1}{2} \left(r_2 e^{-it} + \frac{1}{r_2} e^{it} \right), \quad 0 \leq t \leq 2\pi,$$

where $r_1 > r_2 > 1$. The domain G is the image of the ring $q = r_2/r_1 < |\zeta| < 1$ under the Joukowski map

$$z = \Phi(\zeta) = \frac{1}{2} \left(r_1 \zeta + \frac{1}{r_1 \zeta} \right).$$

Hence, the exact value of conformal capacity of G is given by $\text{cap}(G) = 2\pi / \log(1/q) = 2\pi / \log(r_1/r_2)$.

We use the MATLAB function `annq` with $\alpha = ((r_1 + 1/r_1) + (r_2 + 1/r_2))/4 \in G$, $z_2 = 0$, and $n = 2^{12}$ to compute approximate values for the capacity for several values of r_1 and r_2 . First, we fixed $r_2 = 2$ and chose values of r_1 between 2.05 and 6. The relative errors for the computed values are presented in Figure 3 (left). Then, we fixed $r_1 = 4$ and chose values of r_2 between 1.01 and 3.9. The relative errors for the computed values for this case are presented in Figure 3 (right).

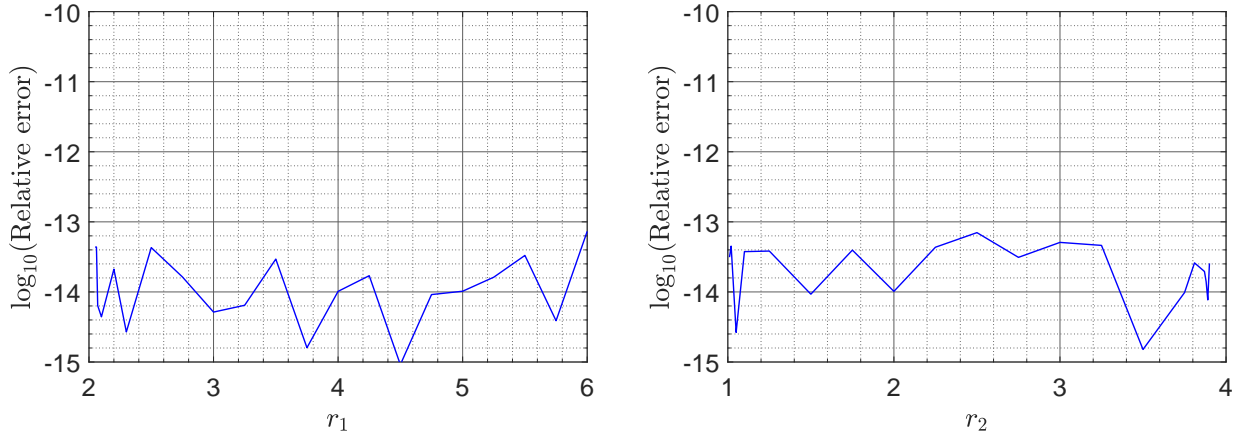


FIGURE 3. Results for the two confocal ellipses domain: Relative errors of the computed conformal capacity for fixed $r = 1$ (left) and fixed $a = 4$ (right).

3.3. Complete elliptic integrals. We recall the following facts about complete elliptic integrals and hypergeometric functions, needed for the sequel. The *Gaussian hypergeometric function* is the analytic continuation to the slit plane $\mathbb{C} \setminus [1, \infty)$ of the series

$$(3.4) \quad F(a, b; c; z) = {}_2F_1(a, b; c; z) = \sum_{n=0}^{\infty} \frac{(a, n)(b, n)}{(c, n)} \frac{z^n}{n!}, \quad |z| < 1.$$

where a, b , and c are complex numbers with $c \neq 0, -1, -2, \dots$. Here $(a, 0) = 1$ for $a \neq 0$, and (a, n) is the *Appell symbol* or the *shifted factorial function*

$$(a, n) = a(a+1)(a+2) \cdots (a+n-1)$$

for $n \in \mathbb{N} \setminus \{0\}$, where $\mathbb{N} = \{0, 1, 2, \dots\}$. The *complete elliptic integrals*, $K(r)$ and $K'(r)$, of the first kind are

$$(3.5) \quad K(r) = \frac{\pi}{2} F(1/2, 1/2; 1; r^2), \quad K'(r) = K(r'), \quad \text{and } r' = \sqrt{1-r^2}.$$

The *elliptic integrals*, $E(r)$ and $E'(r)$, of the second kind are

$$(3.6) \quad E(r) = \frac{\pi}{2} F(1/2, -1/2; 1; r^2), \quad E'(r) = E(r'), \quad \text{and } r' = \sqrt{1-r^2}.$$

Then $K: (0, 1) \rightarrow (0, \infty)$ is an increasing homeomorphism and $E: (0, 1) \rightarrow (1, \pi/2)$ is a decreasing homeomorphism. The decreasing homeomorphism $\mu: (0, 1) \rightarrow (0, \infty)$ is defined by

$$(3.7) \quad \mu(r) \equiv \frac{\pi}{2} \frac{K'(r)}{K(r)}.$$

The basic properties of these functions can be found in [AVV, BF, OLBC]. For example, it follows from [AVV, (5.2)] for $0 < r < 1$ that

$$(3.8) \quad \mu(r) = 2\mu\left(\frac{2\sqrt{r}}{1+r}\right), \quad \mu(r) = \frac{1}{2}\mu\left(\frac{1-r'}{1+r'}\right).$$

In the numerical calculations in this paper, we compute the values of $\mu(r)$ through (3.7) where the values of $K(r)$ and $K'(r)$ are computed by the MATLAB function `ellipke`. Since $0 < r < 1$ and $r' = \sqrt{1-r^2}$, we can show that

$$r < \frac{2\sqrt{r}}{1+r} < 1 \quad \text{and} \quad 0 < \frac{1-r'}{1+r'} < r.$$

Thus, when r is too close to 0, we can use the first formula in (3.8) to get accurate results with MATLAB function `ellipke`. When r is very close to 1, we use the second formula in (3.8).

3.9. Jacobi's inversion formula for μ . In his fundamental work on elliptic functions, C.G.J. Jacobi proved several dozens of formulas for these functions and related functions involving infinite products or theta functions. As pointed out in [AVV, Thm 5.24(2)], some of these formulas can be rewritten so as to give formulas for $\mu^{-1}(y)$. We give two examples. Jacobi's inversion formula for μ is [AVV, Thm 5.24(2)]

$$\mu^{-1}(y)^2 = 1 - \prod_{n=1}^{\infty} \left(\frac{1 - q^{2n-1}}{1 + q^{2n-1}} \right)^8, \quad q = \exp(-2y), \quad y > 0.$$

Another example of Jacobi's work is the following formula for $\mu^{-1}(y)$ in terms of theta functions

$$(3.10) \quad \mu^{-1}(y) = \left(\frac{\theta_2(0, q)}{\theta_3(0, q)} \right)^2, \quad q = \exp(-2y), \quad y > 0,$$

$$(3.11) \quad \theta_2(0, q) = 2 \sum_{n=0}^{\infty} q^{(n+1/2)^2}, \quad \theta_3(0, q) = 1 + 2 \sum_{n=1}^{\infty} q^{n^2}.$$

Because these theta functions converge very fast in $[0, 0.95]$, a few terms of series expansion are enough to achieve numerical values correct up to 15 decimal places. A Newton algorithm for computing $\mu^{-1}(y)$ was implemented in [AVV, pp. 92, 438].

3.12. Square in square. In our third example, we consider the doubly connected domain G which is the difference of two concentric squares

$$((-2, 2) \times (-2, 2)) \setminus ((-2a, 2a) \times (-2a, 2a))$$

where $0 < a < 1$.

The exact value of the capacity of this domain is given by [Bo, pp. 103-104]

$$(3.13) \quad \text{cap}(G) = \frac{4\pi}{\mu(r)},$$

TABLE 1. The approximate values of the capacity for the square in square domain.

a	Our Method	[HRV1]	Exact value	Time (sec)
0.1	2.83977741905231	2.83977741905223	2.83977741905224	6.6
0.2	4.13448702423319	4.134487024234081	4.13448702423409	6.5
0.3	5.63282800094106	5.632828000941654	5.63282800094165	6.5
0.4	7.56153153980938	7.5615315398105745	7.56153153981058	7.1
0.5	10.2340925693693	10.23409256936805	10.2340925693681	7.1
0.6	14.2348796758222	14.234879675824363	14.2348796758244	6.6
0.7	20.9015816764098	20.901581676413954	20.901581676414	6.4
0.8	34.2349151987643	34.23491519877346	34.2349151987734	6.9
0.9	74.2349151987441	74.23491519877882	74.2349151987788	6.9

where

$$c = \frac{1-a}{1+a}, \quad u = \mu^{-1}\left(\frac{\pi c}{2}\right), \quad v = \mu^{-1}\left(\frac{\pi}{2c}\right), \quad r = \left(\frac{u-v}{u+v}\right)^2.$$

Then, by [AVV, Exercises 5.8(3)], we have

$$u^2 + v^2 = \left(\mu^{-1}\left(\frac{\pi c}{2}\right)\right)^2 + \left(\mu^{-1}\left(\frac{\pi^2/4}{\pi c/2}\right)\right)^2 = 1$$

and hence

$$r = \frac{1-2uv}{1+2uv}.$$

By [AVV, (5.2)], we have

$$\mu(2uv)\mu(r) = \mu(2uv)\mu\left(\frac{1-2uv}{1+2uv}\right) = \frac{\pi^2}{2}.$$

Thus, it follows from (3.13) that

$$(3.14) \quad \text{cap}(G) = \frac{8}{\pi}\mu(2uv),$$

We use the MATLAB function `annq` with $\alpha = 1+a \in G$, $z_2 = 0$, and $n = 2^{17}$ to compute approximate values for the capacity for several values of a between 0.1 and 0.9. The obtained results are presented in Table 1. Table 1 presents also the exact values of the capacity and the numerical results computed in [HRV1] using an hp -FEM algorithm. We see from the results presented in the table that accurate results can be obtained using the presented method. The last column in Table 1 presents the CPU time (in seconds) for our method. The GMRES requires between 23 to 25 iterations only to converge. The obtained results using the presented method are not as accurate as the results obtained by the hp -FEM algorithm in [HRV1]. This is expected when we compare BIM and FEM for domains with corners.

3.15. Polygon in polygon. In the forth example, we consider the doubly connected domain G between two polygons. We assume that both polygons have m vertices where

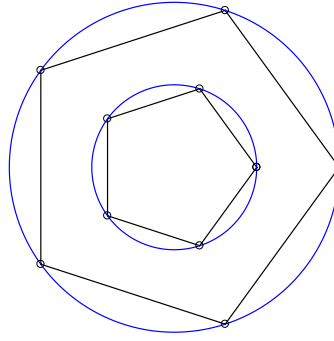


FIGURE 4. The polygon in polygon domain G for $m = 5$ and $q = 0.5$. The figure shows also the annulus $q < |z| < 1$ where the vertices of the two polygons are on the circles $|z| = 1$ and $|z| = q$.

TABLE 2. The approximate values of the capacity for the polygon in polygon domain.

m	Our Method	[BSV]	Time (sec)
3	12.4411574383	12.4412	4.0
4	10.2340925693267		2.5
5	9.62720096044514	9.6266	2.6
7	9.25977557690559	9.2598	2.4
9	9.15441235751744	9.1541	2.1
15	9.08360686195382		1.8
30	9.06705650051687		1.5

$m \geq 3$. We assume that the vertices of the external polygon are the roots of the unity and hence lie on the unit circle $|z| = 1$. For the inner polygon, we assume that the vertices are the roots of the unity multiplied by $q = 0.5$ and thus lie on the circle $|z| = q$ (see Figure 4 for $m = 5$).

The exact value of capacity of the domain is unknown (except for $m = 4$ where the capacity can be computed as in the square in square example, which for $q = 0.5$, is 10.2340925693681). We use the MATLAB function `annq` with $\alpha = (1 + q)/2 \in G$, $z_2 = 0$, and $n = 40320$ to compute approximate values for the capacity for several values of m . The computed capacity is presented in Table 2. As we can see from the table, as m increases, the capacity approaches the capacity of the annulus $q < |z| < 1$ which is $2\pi/\log(1/q)$. For $q = 0.5$, the capacity of the annulus is 9.064720283654388. For some values of m , Table 2 presents also approximate values of the capacity from [BSV]. The last column in Table 2 presents the CPU time (in seconds) for our method.

4. COMPLEMENT OF TWO SLITS

In this section, we consider the doubly connected domain Ω whose complementary components are the two nonintersecting segments $E = [a, b]$ and $F = [c, d]$ where a, b, c and d are complex numbers (see Figure 5 (left) for $a = 0$, $b = 1$, $c = 1 - i$ and $d = 3 + 2i$).



FIGURE 5. The two segments domain Ω for $a = 0$, $b = 1$, $c = 1 - i$ and $d = 3 + 2i$ (left) and the preimage domain G bordered by ellipses (right).

Computing the capacity of such domain Ω has been considered recently in [DNV] using Weierstrass elliptic functions. Here, we shall compute the capacity of Ω using the method presented in Section 2. However, a direct application of the method presented in Section 2 is not possible since the boundaries of Ω are not Jordan curves. So, we need to first map this domain Ω onto a domain G of the forms considered in Section 2. Up to the best of our knowledge, there is no analytic formula for a conformal mapping from the above doubly connected domain Ω onto a doubly connected domain G bordered by smooth Jordan curves. So, we need to use numerical methods to find such an equivalent domain G . An iterative method for computing such a domain G has been presented recently in [NG]. Using this iterative method, a conformally equivalent domain G bordered by ellipses can be obtained as in Figure 5 (right). For details on this iterative numerical method for computing the domain G , we refer the reader to [NG]. For the new domain G , we use the MATLAB function `annq` with $n = 2^{11}$ to compute the capacity of G for several values of the constants a , b , c and d , as in the following examples.

4.1. Two segments on the real axis. When $E = [0, 1]$ and $F = [c, d]$ with $d > c > 1$ are real numbers, the exact capacity of Ω is known and is given by [V2, 5.54 (1), 5.60(1)]

$$(4.2) \quad \frac{\pi}{\mu \left(\sqrt{\frac{d-c}{c(d-1)}} \right)}.$$

We tested our methods for several values of c and d . First, we fixed $c = 2$ and chose d between 2.1 and 10. Then we fixed $c = d - 1$ and chose d between 2.1 and 10. The relative errors of the computed values for this case are presented in Figure 6. As we can see from Figure 6, the presented method gives accurate results with relative error around 10^{-14} . Table 3 presents the approximate values of the capacity, the exact values of the capacity, and the total CPU time for several values of c and d .

4.3. Two vertical segments. The case $E = [a, \bar{a}]$ and $F = [c, \bar{c}]$, with $\text{Im } a \neq 0$ and $\text{Im } c \neq 0$, has been considered in [BBG, Figure E]. We use our method to compute the capacity for the same values of a and c that considered in [BBG, Table 3]. A comparison

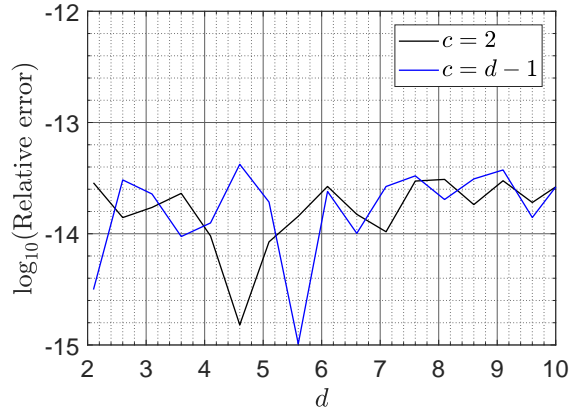


FIGURE 6. Relative errors of the computed conformal capacity for ring domains with complementary components $[0, 1]$ and $[c, d]$, $2.1 \leq d \leq 10$.

TABLE 3. The approximate values of the capacity $\text{cap}([0, 1], [c, d])$.

c	d	Computed value	Exact value	Relative Error	Time (sec)
1.1	2	2.78768694945386	2.7876869494539	1.3×10^{-14}	3.8
1.1	5	3.11161184032646	3.11161184032641	1.7×10^{-14}	7.0
1.1	10	3.19100134481022	3.19100134481039	5.2×10^{-14}	10.0
2	3	1.56340192269607	1.56340192269611	2.7×10^{-14}	1.7
2	5	1.78056882835563	1.78056882835559	1.8×10^{-14}	2.5
2	10	1.9006702400055	1.90067024000545	2.5×10^{-14}	2.9

TABLE 4. The approximate values of the capacity $\text{cap}([a, \bar{a}], [c, \bar{c}])$.

a	c	Our Method	[BBG]	Time (sec)
$0 + i$	$5 + 2i$	1.569943666568835	1.56994325474948999	3.2
$0 + 2i$	$5 + 2i$	1.873067768653831	1.87306699654806386	2.9
$0 + 3i$	$5 + 2i$	2.082038279851203	2.08203777712328096	3.8
$0 + 4i$	$5 + 2i$	2.232598863252026	2.23259828277206300	4.5
$0 + 5i$	$5 + 2i$	2.341589037102932	2.34158897620030515	5.0
$0 + 3i$	$5 + 3i$	2.352412309035929	2.35241226225174034	3.7

of the results computed using our method vs the method presented in [BBG] is given in Table 4 where the last column presents the CPU time for our method.

4.4. **Two general segments.** Finally, let

$$f(a, b, c, d) = \text{cap}([a, b], [c, d]),$$

where a, b, c , and d are complex numbers. We fix $a = 0$ and $b = 4$. Then, for a given point z_1 in the simply connected domain $\hat{\Omega}$ exterior to $[a, b]$, we define the function $u(x, y)$ by

$$u(x, y) = f([0, 4], [z_1, x + iy]) = \text{cap}([0, 4], [z_1, x + iy]).$$

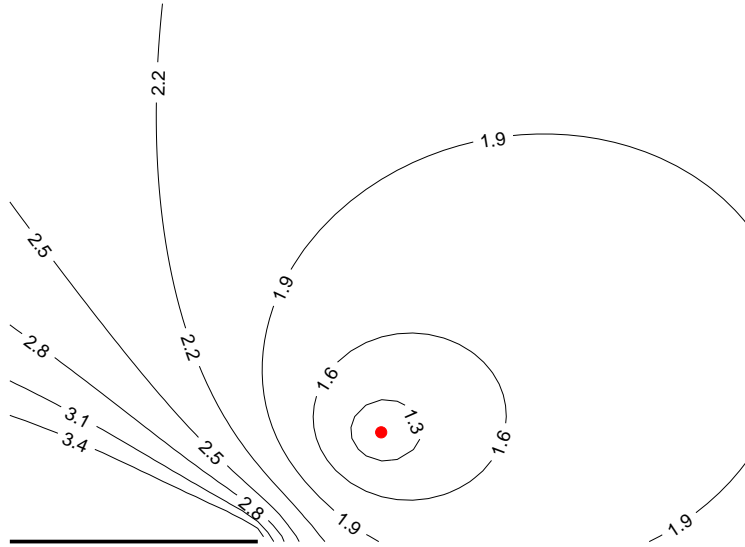


FIGURE 7. Results for the two segments domain: the contour lines of the function $u(x, y) = \text{cap}([0, 4], [6 + 2i, x + iy])$.

TABLE 5. The approximate values of the capacity $\text{cap}([0, 4], [z_1, z_2])$.

$z_2 \setminus z_1$	$6 + 2i$	$6 + 4i$	$6 + 6i$
$1 + i$	4.437462457504561	3.780635179650131	3.564215562104226
$1 + 2i$	3.317286587467568	2.860692915566007	2.711077789477010
$1 + 3i$	2.846059598705353	2.436675855049381	2.295322432200487
$1 + 4i$	2.604420470210280	2.202349785968325	2.046526840859631
$1 + 5i$	2.470153941168786	2.066569200937597	1.886514461888595

for $0 < x < 12$ and $0 < y < 10$ such that the segment $[z_1, x + iy]$ is in $\hat{\Omega}$ with $x + iy \neq z_1$. We plot the contour lines for the function $u(x, y)$ corresponding to several levels. The contour lines for $z_1 = 6 + 2i$, $z_1 = 6 + 4i$, and $z_1 = 6 + 6i$ are shown in Figures 7, 8, and 9, respectively. Table 5 presents the values of the capacity $\text{cap}([0, 4], [z_1, z_2])$ for several values of z_1 and z_2 .

If the interval $[a, b] = [0, 1]$ is considered instead of $[a, b] = [0, 4]$, we obtain the two Figures 10 and 11 for $z_1 = 6 + 4i$ and $z_1 = 5 + 4i$, respectively.

5. RINGS WITH A SEGMENT AS A BOUNDARY COMPONENT

In this section, we shall compute the capacity of doubly connected domains Ω whose boundary components are a slit and a piecewise smooth Jordan curve. Such domains cannot be mapped directly onto an annulus using the method presented in Section 2. To use the method presented in Section 2, we shall use first elementary mappings to map the domain Ω onto a domain G of the types considered in Section 2. Then the domain G is mapped onto an annulus $R = \{z \in \mathbb{C} : q < |z| < 1\}$ and hence the capacity of Ω is

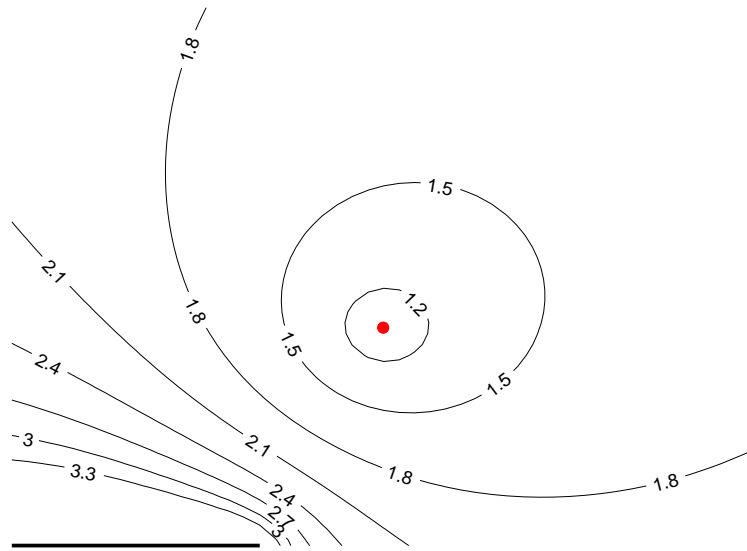


FIGURE 8. Results for the two segments domain: the contour lines of the function $u(x, y) = \text{cap}([0, 4], [6 + 4i, x + iy])$.

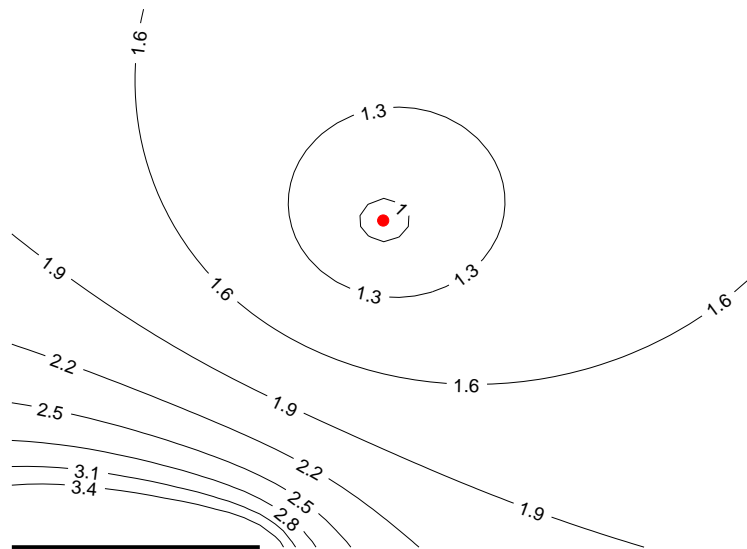


FIGURE 9. Results for the two segments domain: the contour lines of the function $u(x, y) = \text{cap}([0, 4], [6 + 6i, x + iy])$.

$2\pi/\log(1/q)$. In this subsection we consider two examples where the exact value of the capacity for the first example is known.

5.1. Segment and circle. In this example, we consider the doubly connected domain Ω in the exterior of the segment $[0, 1]$ and the circle $|z - a| = r$ where $r > 0$ and a is a real number with $a > 1 + r$ (see Figure 12(left) for $a = 2$ and $r = 0.9$).

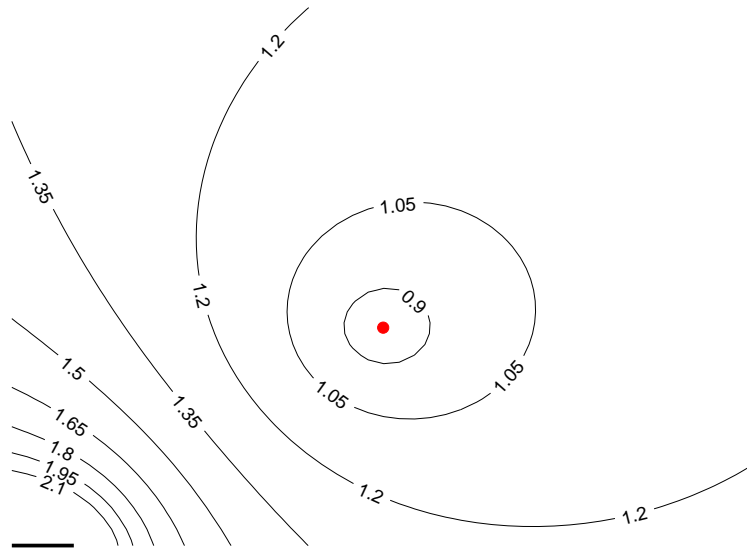


FIGURE 10. Results for the two segments domain: the contour lines of the function $u(x, y) = \text{cap}([0, 1], [6 + 4i, x + iy])$.

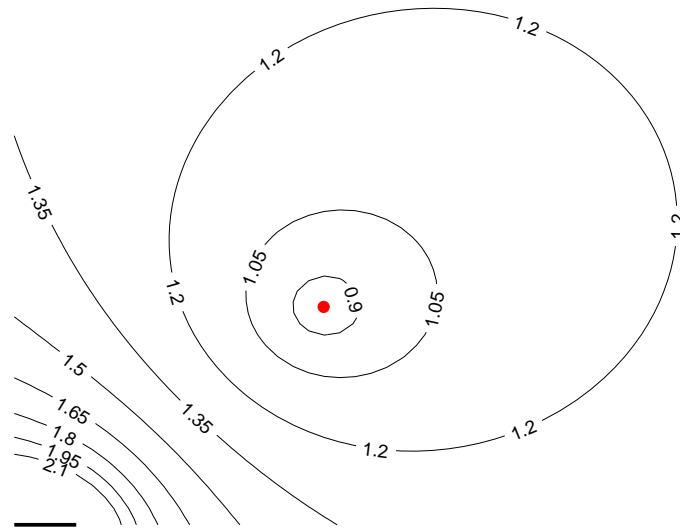


FIGURE 11. Results for the two segments domain: the contour lines of the function $u(x, y) = \text{cap}([0, 1], [5 + 4i, x + iy])$.

The exact value of conformal capacity of the given domain Ω is known and given by [V2, 5.54(2)]

$$(5.2) \quad \text{cap}(\Omega) = \frac{2\pi}{\mu(\tau)}$$

where

$$\tau = \frac{r}{a^2 - a - r^2},$$

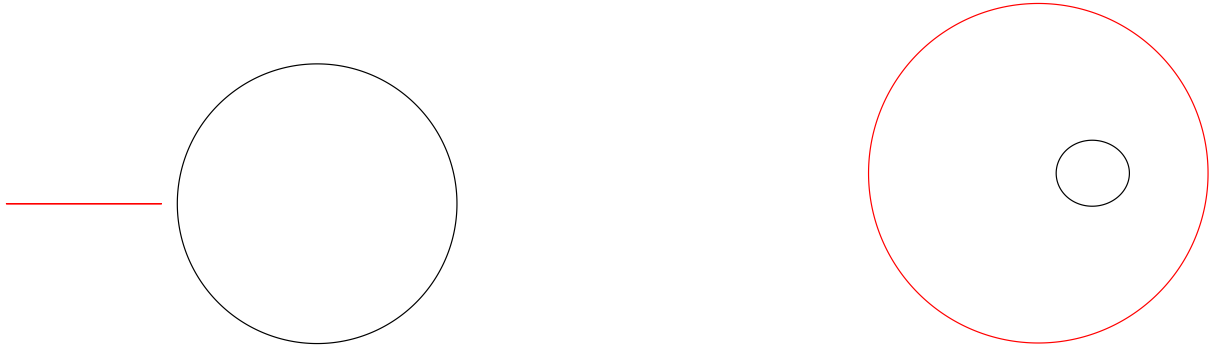


FIGURE 12. The segment and circle domain Ω for $a = 2$ and $r = 0.9$ (left); and the image of this unbounded domain under the mapping $\zeta = \Psi^{-1}(z)$ (right).

and μ is given by (3.7).

To apply our method presented in Section 2, we shall use first elementary mappings to map the domain Ω onto a domain G of the types considered in Section 2. It is known that the function

$$z = \Psi(\zeta) = \frac{1}{4} \left(\zeta + \frac{1}{\zeta} \right) + \frac{1}{2}$$

maps conformally the interior of the unit circle $|\zeta| = 1$ onto the exterior of the segment $[0, 1]$. Hence, its inverse function is given by

$$(5.3) \quad \zeta = \Psi^{-1}(z) = \frac{1}{(2z - 1) \left(1 + \sqrt{1 - \frac{1}{(2z-1)^2}} \right)},$$

where we choose the branch for which $\sqrt{1} = 1$. The function $\zeta = \Psi^{-1}(z)$ maps the segment $[0, 1]$ onto the unit circle $|\zeta| = 1$ and the exterior of the segment $[0, 1]$ onto the interior of the unit circle $|\zeta| = 1$. The function $\zeta = \Psi^{-1}(z)$ maps also the circle $|z - a| = r$ in the z -plane onto a smooth Jordan curve inside the unit circle $|\zeta| = 1$. Consequently, the function $\zeta = \Psi^{-1}(z)$ maps the doubly connected domain Ω onto a bounded doubly connected domain G of the form considered in Section 2 (see Figure 12 (right)).

Then for the domain G , we use the MATLAB function `annq` with $n = 2^{11}$ to compute approximate values for the capacity of Ω for several values of a and r . First, we fixed $r = 1$ and chose values of a between 2.05 and 6. The relative errors of the computed values are presented in Figure 13 (left). Then, we fixed $a = 4$ and chose values of r between 0.05 and 2.95. The relative errors of the computed values for this case are presented in Figure 13 (right). We also presents the approximate values and the exact values of the capacity for several values of r and a in Table 6.

5.4. Segment and ellipse. In connection with the examples presented Subsections 4.1 and 5.1, we consider the following example to show how the capacity of the domains changes when the geometry of the domains changes. Let G_r be the doubly connected domain whose

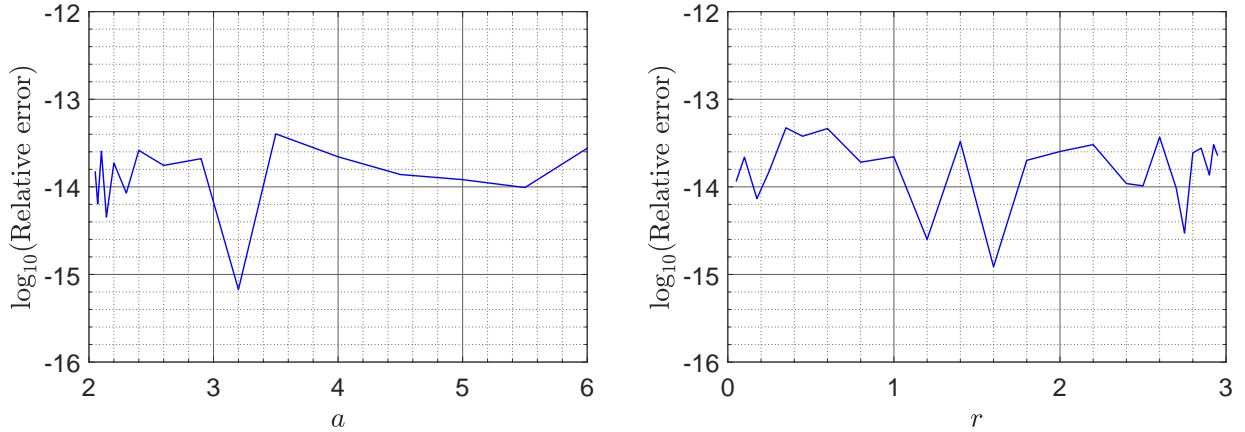


FIGURE 13. Results for the segment and circle domain: Relative errors of the computed conformal capacity for fixed $r = 1$ (left) and fixed $a = 4$ (right).

TABLE 6. The approximate values of the capacity for the segment and circle domain.

r	a	Computed value	Exact value	Relative Error	Time (sec)
0.1	1.2	2.89834979084902	2.89834979084894	2.7×10^{-14}	0.17
0.1	2.2	1.3496258349391	1.34962583493908	1.6×10^{-14}	0.15
0.1	5.2	0.927796431822476	0.927796431822507	3.3×10^{-14}	0.17
1.0	2.1	4.31652297947248	4.31652297947259	2.6×10^{-14}	0.19
3.0	4.1	4.6213142805315	4.62131428053158	1.8×10^{-14}	0.18
5.0	6.1	4.69478341049729	4.69478341049717	2.5×10^{-14}	0.19

complementary components are the two non-intersecting closed sets $E = [0, 1]$ and F_r where F_r is the closed set of points in the interior and on the boundary of the ellipse

$$\eta_r(t) = a + b \cos(t) - ir \sin(t), \quad 0 \leq t \leq 2\pi,$$

where

$$a = \frac{1}{2}(d + c), \quad b = \frac{1}{2}(d - c), \quad 0 < r \leq b < a,$$

and $1 < c < d$ (see Figure 14 (center)).

For $r = 0$, F_r reduced to the segment $F_0 = [c, d]$ and hence G_0 is the doubly connected domain exterior to the two segments $E = [0, 1]$ and $F_0 = [c, d]$ as considered in Subsection 4.1 (see Figure 14 (left)). The exact value of $\text{cap}(E, F_0)$ is given by (4.2), i.e.,

$$(5.5) \quad \text{cap}(E, F_0) = \frac{\pi}{\mu(s)}, \quad s = \sqrt{\frac{d - c}{c(d - 1)}},$$

where μ is given by (3.7).

When $r = b$, F_b is the closed disk $|z - a| \leq b$ and the domain G_b is then the doubly connected domain exterior to the segment $E = [0, 1]$ and the closed disk $F_b = \{x \mid |z - a| \leq b\}$.

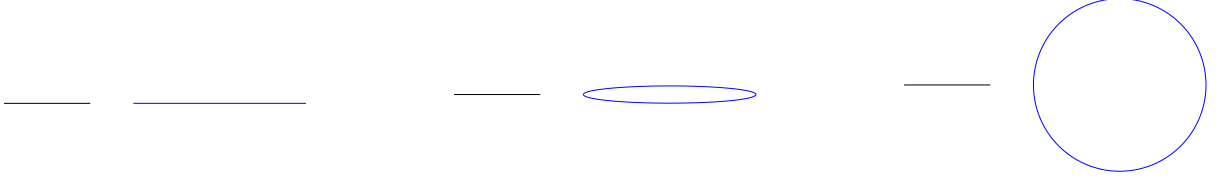


FIGURE 14. The domain G_r with $c = 1.5$, $d = 3.5$ for $r = 0$ (left), $r = 0.1$ (center) and $r = b$ (right).

$b\}$ which considered in Subsection 5.1 (see Figure 14 (right)). The exact value of $\text{cap}(E, F_b)$ is given by (5.2), i.e.,

$$(5.6) \quad \text{cap}(E, F_b) = \frac{2\pi}{\mu(s)}, \quad s = \frac{b}{a^2 - a - b^2}.$$

It is clear from the definition of the closed set F_r that $F_0 \subseteq F_r \subseteq F_b$ for $0 \leq r \leq b$. As r changes continuously from 0 to b , the closed set F_r changes continuously from the segment F_0 to the disk F_b . Here, we shall compute the exact value of the capacity $\text{cap}(E, F_r)$ and show that $\text{cap}(E, F_r)$ will change from $\text{cap}(E, F_0)$ to $\text{cap}(E, F_b)$ as r changes from 0 to b .

By the elementary mapping

$$\zeta = \Psi_1(z) = \frac{z - a}{b},$$

the unbounded domain G is mapped conformally onto the unbounded domain G_1 exterior to the segment $[-a/b, -(a-1)/b]$ and the ellipse

$$\eta_1(t) = \cos(t) - i(r/b) \sin(t), \quad 0 \leq t \leq 2\pi.$$

We can easily show that the function

$$\zeta = \Psi_2(\xi) = \xi + \frac{1 - (r/b)^2}{4} \frac{1}{\xi}$$

maps the domain exterior to the circle $|\xi| = (1 + r/b)/2$ onto the domain exterior of the ellipse. Hence, the inverse mapping

$$\xi = \Psi_2^{-1}(\zeta) = \zeta \left(\frac{1}{2} + \frac{1}{2} \sqrt{1 - \frac{1 - (r/b)^2}{\zeta^2}} \right),$$

maps the domain G_1 onto the domain G_2 exterior to the circle $|\xi| = (1 + r/b)/2$ and the segment $[c_1, d_1]$ where

$$(5.7) \quad c_1 = -\frac{a + \sqrt{a^2 - b^2 + r^2}}{2b}, \quad d_1 = -\frac{a - 1 + \sqrt{(a-1)^2 - b^2 + r^2}}{2b},$$

and the branch of the square root is chosen such that $\sqrt{1} = 1$. Finally, the function

$$w = \Psi_3(\xi) = \frac{\xi - c_1}{d_1 - c_1},$$

maps the domain G_2 onto the domain G_3 exterior to the circle $|w - \hat{a}| = \hat{r}$ and the segment $[0, 1]$ where

$$(5.8) \quad \hat{a} = -\frac{c_1}{d_1 - c_1}, \quad \hat{r} = \frac{b+r}{2b} \frac{1}{d_1 - c_1}.$$

Hence, the analytic value of $\text{cap}(E, F_r)$ can be obtained since the exact value of conformal capacity of the domain G_3 is known [V2,5.54(2)],

$$(5.9) \quad \text{cap}(E, F_r) = \frac{2\pi}{\mu(\tau_r)}$$

where

$$(5.10) \quad \tau_r = \frac{\hat{r}}{\hat{a}^2 - \hat{a} - \hat{r}^2}.$$

The value of τ_r can be obtained in terms of c , d and r as following

$$\tau_r = \frac{2(d-c+2r)(1 + \sqrt{dc+r^2} - \sqrt{dc-d-c+1+r^2})}{(d+c+2\sqrt{dc+r^2})(d+c-2+2\sqrt{dc-d-c+1+r^2}) - (d-c+2r)^2}.$$

For $r = 0$, the capacity given by (5.9) becomes

$$(5.11) \quad \frac{2\pi}{\mu(\tau_0)}$$

where

$$(5.12) \quad \begin{aligned} \tau_0 &= \frac{2(d-c)(1 + \sqrt{dc} - \sqrt{dc-d-c+1})}{(d+c+2\sqrt{dc})(d+c-2+2\sqrt{dc-d-c+1}) - (d-c)^2} \\ &= \frac{\sqrt{d}-\sqrt{c}}{\sqrt{d}+\sqrt{c}} \frac{\sqrt{cd}-\sqrt{(c-1)(d-1)}+1}{\sqrt{cd}+\sqrt{(c-1)(d-1)}-1} \end{aligned}$$

After tedious algebra, we find that s in (5.5) is related to τ_0 in (5.12) through

$$(5.13) \quad s = \frac{2\sqrt{\tau_0}}{1 + \tau_0},$$

which, in view of (3.8), implies that

$$\mu(\tau_0) = 2\mu(s).$$

Hence,

$$\text{cap}(E, F_0) = \frac{\pi}{\mu(s)} = \frac{2\pi}{\mu(\tau_0)}$$

and thus the capacity $\text{cap}(E, F_r)$ given by (5.9) reduced to the capacity $\text{cap}(E, F_0)$ for $r = 0$. Furthermore, when $r = b$, then it follows from (5.7) and (5.8) that $\hat{a} = a$ and $\hat{r} = r = b$. Hence, it follows from (5.10) that

$$\tau_b = \frac{r}{a^2 - a - r^2},$$

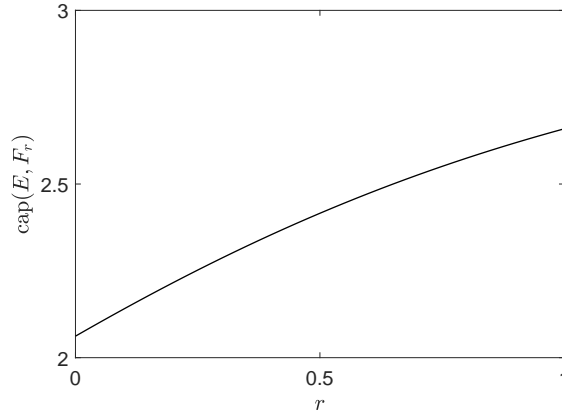


FIGURE 15. The values of $\text{cap}(E, F_r)$ for $c = 1.5$, $d = 3.5$, $0 \leq r \leq b$.



FIGURE 16. The segment and polygon domain Ω for $a = 1.6$ and $r = 0.5$ (left); and the image of this unbounded domain under the mapping $\zeta = \Psi^{-1}(z)$ (right).

which implies that the capacity $\text{cap}(E, F_r)$ given by (5.9) reduced to the Formula (5.6) for $r = b$.

The values of $\text{cap}(E, F_r)$ for $c = 1.5$, $d = 3.5$, $0 \leq r \leq b$ (where $b = (d-c)/2 = 1$) is given in Figure 15. As we can see from Figure 15, the capacity $\text{cap}(E, F_r)$ changes continuously and rapidly increases from $\text{cap}(E, F_0)$ to $\text{cap}(E, F_b)$ as r changes continuously from 0 to b .

5.14. Segment and polygon. In this example, we consider the doubly connected domain Ω in the exterior of the segment $[0, 1]$ and a polygon with m vertices where $m \geq 3$. We assume that the vertices of the polygon are given by

$$v_k = a - re^{\frac{-2k\pi i}{m}}, \quad k = 0, 1, 2, \dots, m-1$$

(see Figure 16 (left) for $a = 1.6$, $r = 0.5$, and $m = 3$).

The exact value of conformal capacity is unknown. To use the method presented in Section 2, we first use the mapping function $\zeta = \Psi^{-1}(z)$ in Subsection 5.1 to map the doubly connected domain Ω in the exterior of the segment $[0, 1]$ and the polygon onto a

r	a	m	Capacity (segment and polygon)	Capacity (segment and circle)
1	2.1	3	3.385465691885468	4.31652297947259
		8	3.996010644504850	
		16	4.198837938505387	
		128	4.314154067689326	
0.5	4	3	1.291427925789600	1.38309579015095
		8	1.368162812590014	
		16	1.379193284259540	
		128	1.383032359435526	
2.5	10	3	1.199970598794575	1.28290663972126
		8	1.268817744415183	
		16	1.279211726247828	
		128	1.282846509334037	

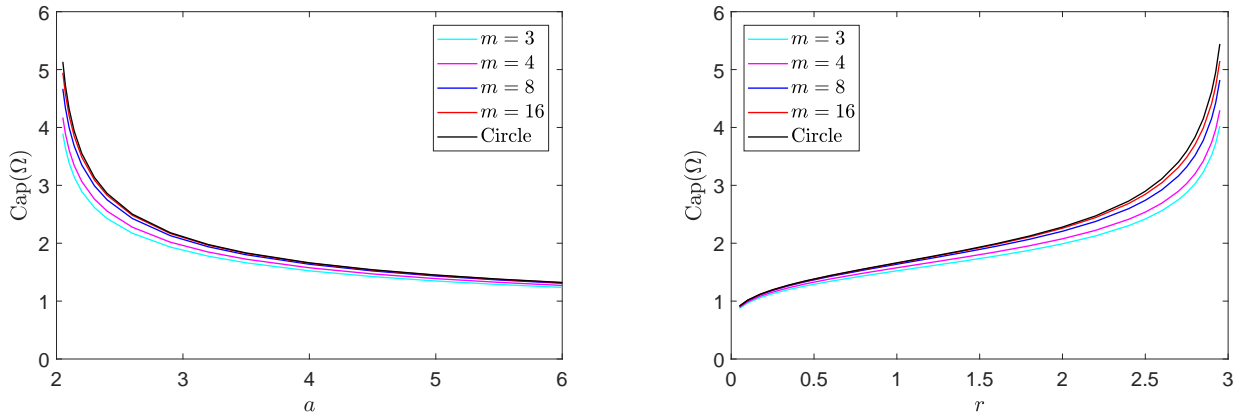


FIGURE 17. Results for the segment and polygon domain: The computed conformal capacity for fixed $r = 1$ (left) and fixed $a = 4$ (right).

bounded doubly connected domain G of the form we considered in Section 2 (see Figure 16 (right)). Then, for the new domain G , we use the MATLAB function `annq` with $n = 15 \times 2^9$ to compute approximate values for the capacity of Ω for several values of m , a and r . First, we fixed $r = 1$ and chose values of a between 2.05 and 6. The computed capacity for $m = 3, 4, 8, 16$ are presented in Figure 17 (left). Then, we fixed $a = 4$ and chose values of r between 0.05 and 2.95. The computed capacity for $m = 3, 4, 8, 16$ are presented in Figure 17 (right). Figure 17 presents also the capacity for the segment with circle domain in the previous examples for the same values of a and r . The following table presents the values of the capacity for the segment with circle domain and for the segment with polygon domain for several values of a , r , and m . As we can see from the presented results, the capacity of the segment and polygon domain approaches the the capacity of the segment and circle domain as the number of vertices m increases.

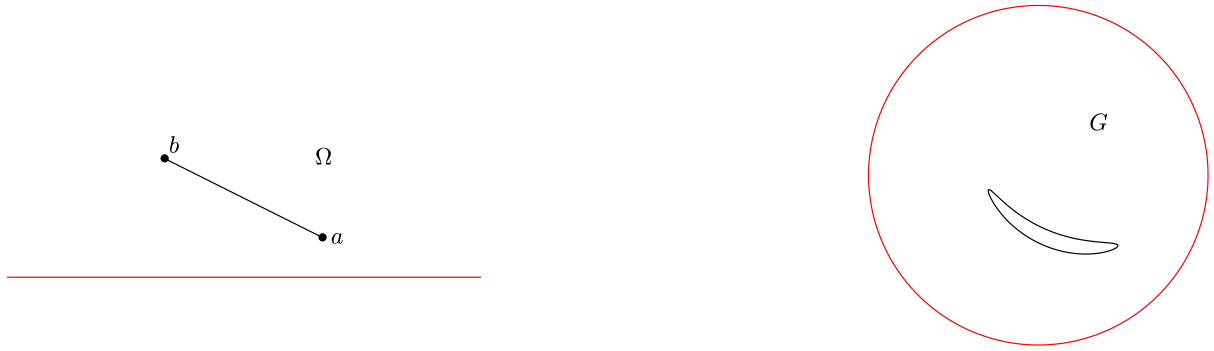


FIGURE 18. The half-plane with a segment domain Ω for $a = 1 + 0.5i$ and $b = -1 + 1.5i$ (left) and the preimage domain G bordered by smooth Jordan curves (right).

6. THE UPPER HALF-PLANE WITH A SLIT

In this section, we consider the doubly connected domain $\Omega = \mathbb{H}^2 \setminus [a, b]$ where \mathbb{H}^2 is the upper half-plane $\{z \in \mathbb{C} : \text{Im}(z) > 0\}$ and, a and b are two complex numbers in \mathbb{H}^2 (see Figure 18 (left)).

The method presented in Section 2 is not directly applicable to such domains Ω . So, we first map this domain to a domain G of the forms considered in Section 2. Since there is no exact conformal mapping from the domain Ω onto a doubly connected domain G bordered by smooth Jordan curves, we find such equivalent domain G using numerical methods. An iterative numerical method for computing such domain G has been presented in [NG]. We will omit the details here about the iterative method and refer the reader to [NG]. Using this iterative method, for a give half-plane with a segment domain Ω , a conformally equivalent domain G bordered by smooth Jordan curves can be obtained as in Figure 18 (right). For the new domain G , we use the MATLAB function `annq` with $n = 2^{11}$ to compute the capacity of the given domain Ω .

For the segment $F = [si, ri]$ where $r > s > 0$ are real numbers, the exact capacity of Ω is known and is given by [V2, (5.56), Theorem 8.6 (1)]

$$(6.1) \quad \frac{2\pi}{\mu\left(\tanh\left(\frac{1}{2}\log\frac{r}{s}\right)\right)}.$$

We tested our methods for several values of s and r . First, we chose the vertical segment $F = [si, (1+s)i]$, i.e., $a = si$ and $b = (1+s)i$, for $0.05 \leq s \leq 6$. The relative errors of the computed values of the capacity for this case are presented in Figure 19. We see from Figure 19 that the presented method gives accurate results with relative error around 10^{-14} . The approximate values of the capacity, the exact values of the capacity, and the total CPU time for several values of s and r are presented in Table 7.

We also compute the values of the capacity for the vertical segment $F = [(3-s)i, (3+s)i]$ for $0.05 \leq s \leq 2.95$ and for the horizontal segment $F = [-s+3i, s+3i]$ for $0.05 \leq s \leq 3$. Both segments pass through the point $3i$ and have the length $2s$. The results are presented

TABLE 7. The approximate values of the capacity $\text{cap}(\Omega)$ for $\Omega = \mathbb{H}^2 \setminus [si, ri]$.

s	r	Computed value	Exact value	Relative Error	Time (sec)
0.1	1	4.69363108974789	4.6936310897475	8.2×10^{-14}	2.9
0.1	5	6.74589984699685	6.74589984699653	4.8×10^{-14}	5.3
0.1	10	7.62853775997519	7.62853775997481	5.0×10^{-14}	6.6
1	2	2.55852314234207	2.55852314234201	2.1×10^{-14}	2.2
1	5	3.80134048001095	3.80134048001091	1.7×10^{-14}	2.6
1	10	4.6936310897476	4.6936310897475	2.1×10^{-14}	3.1

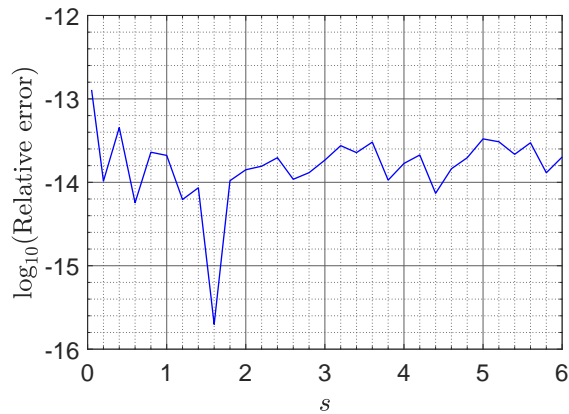
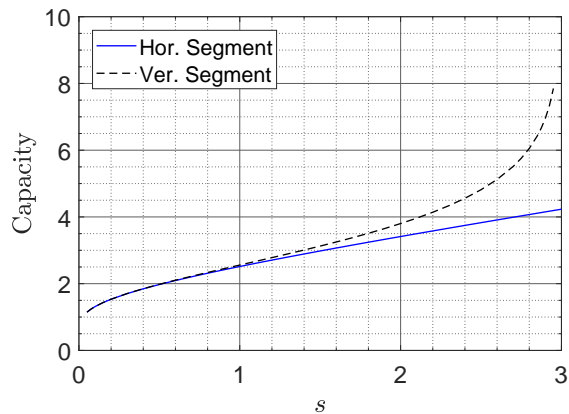
FIGURE 19. Results for the half-plane with a segment domain: Relative errors of the computed conformal capacity for the segment $F = [si, (1 + s)i]$ for $0.05 \leq s \leq 6$.

FIGURE 20. Results for the half-plane with a segment domain: The computed capacities.

in Figure 20. As we can see from Figure 20, the capacity increases as the length of the segment increases. For vertical segment, the capacity increases more rapidly when the segment becomes close to the real line.

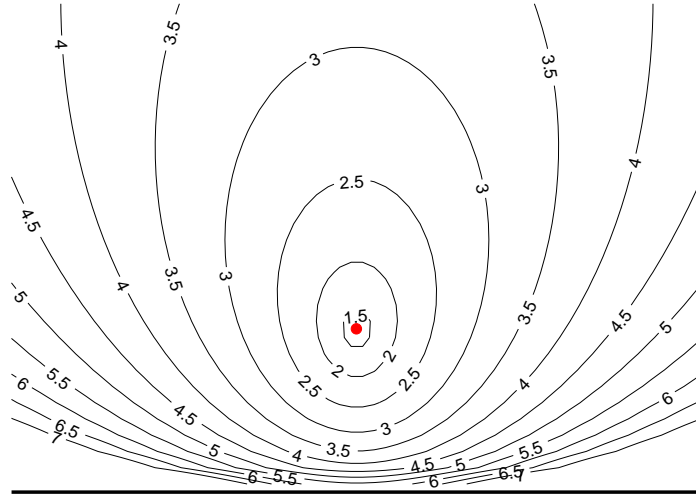


FIGURE 21. Results for the half-plane with a segment domain: the contour lines of the function $u(x, y) = \text{cap}(\mathbb{H}^2 \setminus [i, x + iy])$.

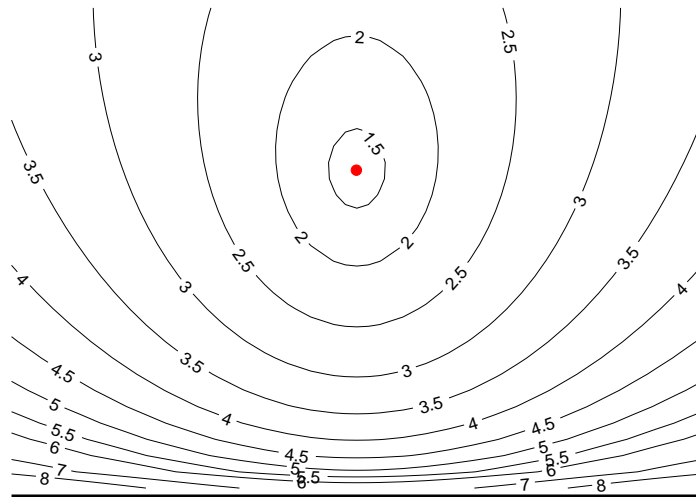


FIGURE 22. Results for the half-plane with a segment domain: the contour lines of the function $u(x, y) = \text{cap}(\mathbb{H}^2 \setminus [2i, x + iy])$.

Finally, for a given point z_1 in \mathbb{H}^2 , we define the function $u(x, y)$ by

$$u(x, y) = \text{cap}(\mathbb{H}^2 \setminus [z_1, x + iy])$$

for $-3 < x < 3$ and $0 < y < 3$ such that $x + iy \neq z_1$. We plot the contour lines for the function $u(x, y)$ corresponding to several levels. The contour lines are shown in Figures 21 for $z_1 = i$ and in Figures 22 for $z_1 = 2i$.

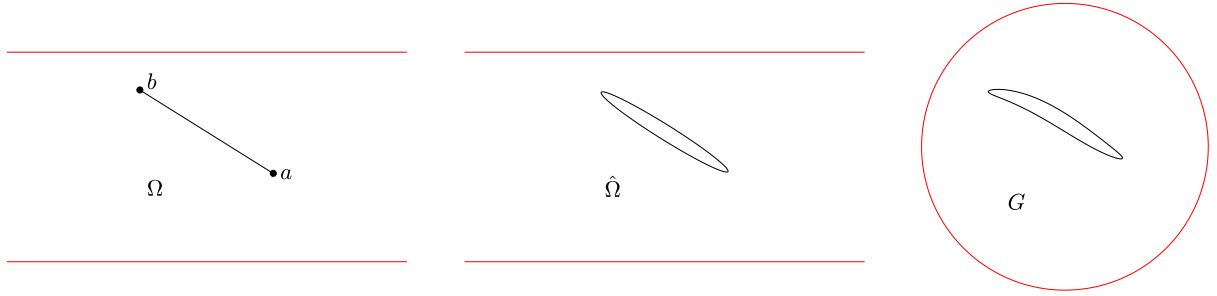


FIGURE 23. The given strip with a segment domain Ω for $a = 1 - 0.25i$ and $b = -1 + i$ (left), the intermediate domain $\hat{\Omega}$ (center), and the computed preimage domain G (right).

7. A STRIP WITH A SLIT

In this section, we consider the doubly connected domain $\Omega = S \setminus F$ where S is the infinite strip $|\operatorname{Im} z| < \frac{\pi}{2}$, $a, b \in S$, and F is the segment $[a, b]$ (see Figure 23(left)).

Similar to the domains considered in Sections 4 and 6, the method presented in Section 2 is not directly applicable to the domain $\Omega = S \setminus F$ described above. Thus, we first map this domain onto an equivalent domain G of the forms considered in Section 2, i.e., a domain bordered by smooth Jordan curves ((see Figure 23(right)).

For the two domains considered in the Sections 4 and 6, we used the iterative method presented in [NG] to find equivalent domains bordered by smooth Jordan curves. Similar iterative methods have been presented in [N4] for other canonical slit domains. However, the canonical domain $\Omega = S \setminus F$ obtained by removing a segment F from the infinite strip S has not been considered in [NG, N4]. So, for the domain Ω , we shall present in the next subsection an iterative method for computing an equivalent doubly connected domain G bordered by smooth Jordan curves. The iterative method is similar to the iterative methods presented in [AST, NG, N4].

7.1. A preimage domain for a strip with a slit domain. Let G be the doubly connected domain in the interior of the unit circle Γ_1 and the exterior of a smooth Jordan curve Γ_2 . Let also Ω be the canonical domain consisting of the strip $|\operatorname{Im} z| < \pi/2$ with a slit L along a straight line such that the angle between the line and the positive real axis is θ_2 ; see Figure 23 (left). An efficient numerical method for computing the conformal map $z = \Phi(\zeta)$ from G onto the domain Ω such that

$$(7.2) \quad \Phi(1) = \infty + i0, \quad \Phi(i) = \frac{\pi}{2}i \quad \text{and} \quad \Phi(-1) = -\infty + i0$$

has been presented in [NF]. The center and the length of the slit L depend uniquely on the given domain G . Assume that $\Gamma = \partial G$ is parametrized by a function $\eta(t)$ as in (2.5). Assume also $\theta_1 = 0$, θ_2 is the angle between the slit L and the positive real axis, the function A be defined by (2.6); and the operators \mathbf{N} and \mathbf{M} are as in Subsection 2.3. Then, the following theorem from [NF] provides us with a method for computing the conformal mapping from the domain G onto the domain Ω .

Theorem 7.3. Let $\theta_1 = 0$, let θ_2 be the angle between the slit L and the positive real axis, let the function A be defined by (2.6), and let the function γ be defined by

$$(7.4) \quad \gamma(t) = \begin{cases} 0, & t \in J_1, \\ \operatorname{Im} [e^{-i\theta_2} \Psi(\eta(t))], & t \in J_2, \end{cases}$$

where the function Ψ is defined by

$$(7.5) \quad \Psi(\zeta) = \log \frac{1 + \zeta}{1 - \zeta}.$$

If ρ is the unique solution of the boundary integral equation (2.9) and the piecewise constant function h is given by (2.10), then the conformal mapping Φ from G onto Ω is given by

$$(7.6) \quad \Phi(\zeta) = -if(i) + \zeta f(\zeta) + \Psi(\zeta), \quad \zeta \in G \cup \Gamma,$$

where f is the analytic function in G with the boundary values (2.11).

In Theorem 7.3, the domain G is assumed to be given and the canonical domain Ω is to be found. The integral equation (2.9) is then used to find the domain Ω and the conformal map $z = \Phi(\zeta)$ from G onto Ω . In our application, however, we assume that the domain Ω (strip with slit) is given and we want to find the domain G . For such case, a direct application of Theorem 7.3 is not possible. So, similar to the iterative methods presented in [AST, NG, N4], we will describe in this subsection an iterative method to compute the (unknown) preimage domain G and the conformal map $z = \Phi(\zeta)$ from the domain G onto the (known) strip with a slit domain Ω such that Φ satisfies the normalization conditions (7.2).

For a given doubly connected domain Ω consisting of the strip $|\operatorname{Im} z| < \pi/2$ with a rectilinear slit L , let $|L|$ denote the length of the slit L , ζ_L denotes its center, and θ_2 denotes the angle between the positive real axis and the slit L . For $k = 0, 1, 2, 3, \dots$, where k denotes the iteration number, let $\hat{\Omega}^k$ be the doubly connected domain in the strip $|\operatorname{Im} \xi| < \pi/2$ and in the exterior of the ellipse \hat{L}^k parametrized by

$$\hat{\eta}^k(t) = \hat{z}^k + 0.5a^k e^{i\theta_2} (\cos t - ir \sin t), \quad t \in J_2,$$

where r is the ratio of the lengths of the major to the minor axes of the ellipse, $0 < r \leq 1$. The parameters \hat{z}^k and a^k of the ellipses will be computed by the iterative method described below. Note that, the domain $\hat{\Omega}^k$ is obtained from Ω by replacing the slit L by a thin ellipse \hat{L}^k whose major axis is on the slit L (see Figure 23 (center)). Then the preimage domain G^k is assumed to be the image of the doubly connected domain $\hat{\Omega}^k$ under the conformal mapping $\zeta = \Psi^{-1}(\xi)$ where Ψ^{-1} is the inverse of the function Ψ in (7.5), i.e.,

$$\zeta = \Psi^{-1}(\xi) = \frac{\exp(\xi) - 1}{\exp(\xi) + 1} = \operatorname{th}(\xi/2),$$

(see Figure 23 (right)). Hence, the preimage domain G^k is the bounded doubly connected domain interior to the unit circle parametrized by

$$\eta_1^k(t) = e^{it}, \quad t \in J_1,$$

and exterior to the quasi-ellipse Γ_2 parametrized by

$$\eta_2^k(t) = \Psi^{-1}(\hat{\eta}^k(t)), \quad t \in J_2.$$

The parameters \hat{z}^k and a^k will be computed as follows:

Initialization:

Set

$$\hat{z}^0 = \zeta_L, \quad a^0 = (1 - 0.5r)|L|, \quad j = 1, 2, \dots, m.$$

Iterations:

For $k = 1, 2, 3, \dots$,

- The preimage domain G^{k-1} is mapped by the method presented in Theorem 7.3 onto the canonical domain Ω^k (the strip $|\operatorname{Im} \zeta| < \pi/2$ with a rectilinear slits L^k making angles θ_2 with the positive real axis).
- Let ζ_L^k be the center of the slit L^k and $|L^k|$ be its length. The parameters of the preimage domain G^k are updated through

$$\begin{aligned} \hat{z}^k &= \hat{z}^{k-1} - (\zeta_L^k - \zeta_L), \\ a^k &= a^{k-1} - (1 - 0.5r)(|L^k| - |L|). \end{aligned}$$

- Stop the iteration if

$$\frac{1}{m} \sum_{j=1}^m (|\zeta_L^k - \zeta_L| + ||L^k| - |L||) < \varepsilon \quad \text{or} \quad k > \mathbf{Max}$$

where \mathbf{Max} is the maximum number of allowed iterations and ε is a given tolerance. In our numerical experiments, we choose $\mathbf{Max} = 100$ and $\varepsilon = 10^{-14}$.

The iterative method produces a sequence of doubly connected domains $G^0, G^1, G^2, G^3, \dots$ which converges to the required preimage domain G bordered by smooth Jordan curves. The iterative method provides us also with a conformal map $z = \Phi(\zeta)$ from G onto the given domain Ω .

Finally, similar iterative methods have been tested in [NG, N4] for other canonical domains. The numerical examples presented in [NG, N4, LSN] show that the iterative method converges after only few number iterations even for domain with high connectivity. However, so far, no proof of convergence is yet available.

7.7. Computing the capacity. For a given domain $\Omega = S \setminus F$, in this example, we use the above iterative method with $n = 2^{11}$ to find an equivalent domain G bordered by smooth Jordan curves. Then we use the MATLAB function `annq` to compute the capacity of G which is equal to the capacity of the given domain Ω . For the segment $F = [0, s]$ where $s > 0$ is a real number, we can find the exact value the capacity of Ω . It is clear that the mapping

$$w = \Phi(z) = \frac{e^z - 1}{e^z + 1} = \operatorname{th}(z/2)$$

maps conformally the strip $-\frac{\pi}{2} < \operatorname{Im} z < \frac{\pi}{2}$ onto the unit disk $|w| < 1$ and maps the segment $F = [0, s]$ onto the segment $[0, \tanh(s/2)]$ on the real line interior to the unit

TABLE 8. The approximate values of the capacity for $\Omega = S \setminus [0, s]$ where S is the infinite strip $|\operatorname{Im} z| < \frac{\pi}{2}$.

s	Computed value	Exact value	Relative Error	Time (sec)
0.1	1.43378560632985	1.4337856063298	3.3×10^{-14}	1.8
0.5	2.2619707501643	2.26197075016437	3.1×10^{-14}	2.0
1	2.99266869365819	2.99266869365819	1.8×10^{-15}	2.0
2	4.30568998739557	4.30568998739557	2.1×10^{-16}	2.4
3	5.58401362841096	5.58401362841108	2.1×10^{-14}	3.0
5	8.1312680736435	8.13126807338401	3.2×10^{-11}	4.5

circle. Then capacity of the domain obtained by removing the real segment $[0, \tanh(s/2)]$ from the unit disk is known and is given by (see [LV], [V2, Thm 8.6(1)])

$$(7.8) \quad \frac{2\pi}{\mu(\tanh \frac{s}{2})}$$

which is also the capacity of the domain Ω by conformal invariance of the capacity. For such a domain, we use our method to compute the capacity for several values of s . The approximate values of the capacity, the exact values of the capacity, and the total CPU time are presented in Table 8.

The presented method is used also to compute approximate values of the capacity for other segments. The computed values of the capacity for the vertical segment $F = [(s - 0.5)i, (s + 0.5)i]$ for $-1.05 \leq s \leq 1.05$ vs s are shown in Figure 24 (left). Figure 24 (left) shows also the computed values of the capacity for the horizontal segment $F = [-0.5 + si, 0.5 + si]$ for $-1.55 \leq s \leq 1.55$. As we can see from Figure 24 (left), the capacity increases as the segment moves vertically toward the lines $\operatorname{Im} z = -\pi/2$ and $\operatorname{Im} z = \pi/2$. Figure 24 (right) shows the computed values of the capacity for the vertical segment $F = [s - 0.5i, s + 0.5i]$ and the horizontal segment $F = [s - 0.5, s + 0.5]$ for $-4 \leq s \leq 4$. As we can see from Figure 24 (right), the capacity does not change as the segment moves horizontally in parallel to the lines $\operatorname{Im} z = -\pi/2$ and $\operatorname{Im} z = \pi/2$. We also compute the values of the capacity for the vertical segment $F = [-si, si]$ and the horizontal segment $F = [-s, s]$ for $0.05 \leq s \leq 1.5$. Both segments passes through the origin and has the length $2s$. The results are presented in Figure 25. As we can see from Figure 20, the capacity increases as the length of the segment increase. For vertical segment, the capacity increases more rapidly when the segment becomes close to the lines $\operatorname{Im} z = -\pi/2$ and $\operatorname{Im} z = \pi/2$.

Finally, for a given point z_1 in S , we define the function $u(x, y)$ by

$$u(x, y) = \operatorname{cap}(S \setminus [z_1, x + iy])$$

for $-3 < x < 3$ and $-\pi/2 < y < \pi/2$ such that $x + iy \neq z_1$. We plot the contour lines for the function $u(x, y)$ corresponding to the several levels. The contour lines are shown in Figures 26 for $z_1 = 0$ and in Figures 27 for $z_1 = i$. Table 9 presents the values of the capacity $\operatorname{cap}(S \setminus [z_1, z_2])$ for several values of z_1 and z_2 .

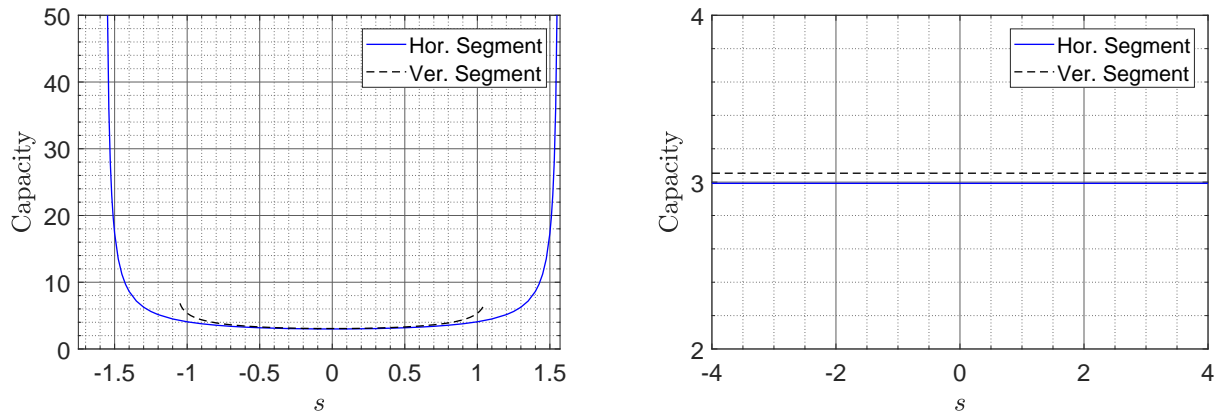


FIGURE 24. Results for the strip with a segment domain: The computed capacities.

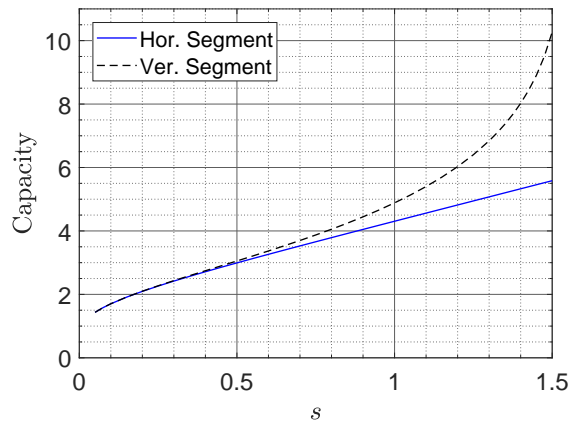


FIGURE 25. Results for the strip with a segment domain: The computed capacities.

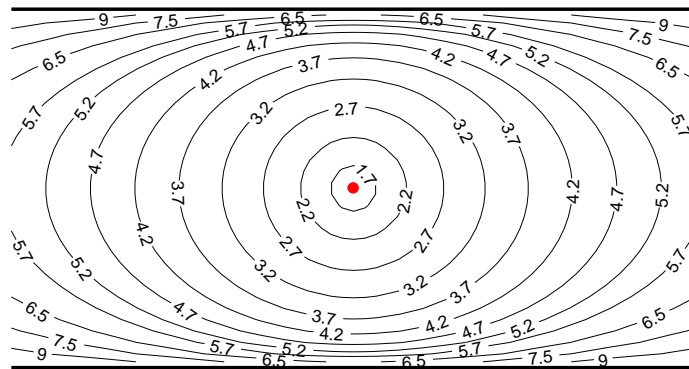


FIGURE 26. Results for the strip with a segment domain: the contour lines of the function $u(x, y) = \text{cap}(S \setminus [0, x + iy])$.

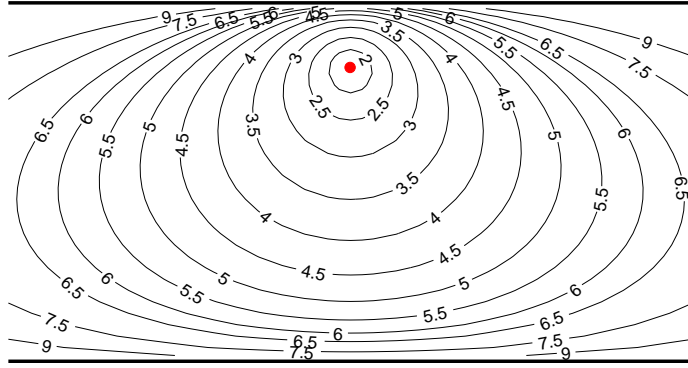


FIGURE 27. Results for the strip with a segment domain: the contour lines of the function $u(x, y) = \text{cap}(S \setminus [i, x + iy])$.

TABLE 9. The approximate values of the capacity $\text{cap}(S \setminus [z_1, z_2])$.

$z_2 \setminus z_1$	0	i
$-2 - i$	5.22039352683477	6.16235340104672
$-1 - i$	3.95535941720605	5.2505796947497
$-i$	3.29790704462477	4.88518878969611
$1 - i$	3.95535941720591	5.2505796947496
$2 - i$	5.22039352683478	6.16235340104709

8. DOMAINS EXTERIOR TO THIN RECTANGLES

8.1. Two rectangles. We consider in this section the doubly connected domain G in the exterior of the rectangular closed sets

$$[0, 1] \times [0.5 - d, 0.5 + d] \quad \text{and} \quad [0, 1] \times [-0.5 - d, -0.5 + d]$$

where $0 < d < 0.5$ (see the Figure 28). We use the MATLAB function `annq` presented in Subsection 2.23 with $n = 2^{15}$ to compute the capacity of G for several values of d .

When $d = 0$, the two rectangles reduced to the two slits $[i/2, 1 + i/2]$ and $[-i/2, 1 - i/2]$. For these two slits, we can use the numerical method presented in Section 4 to compute the capacity of the domain in the exterior to these two slits. The obtained results are presented at the bottom of Table 10.

Let R_1 be the unbounded doubly connected domain in the exterior to the two slits $[i/2, 1 + i/2]$ and $[-i/2, 1 - i/2]$ (corresponding to $d = 0$). The exact value of the capacity of R_1 can be computed. For $0 < k < 1$, consider the unbounded doubly connected domain R_2 in the exterior of the two slits $[-1/k, -1]$ and $[1, 1/k]$. Then the Möbius transform

$$\Psi(z) = \frac{2k}{k-1} \frac{z+1}{kz-1}$$

maps the domain R_2 onto the unbounded doubly connected domain R_3 in the exterior of the two slits $[-1, 0]$ and $[s, +\infty]$ where $s = \Psi(1) = 4k/(1-k)^2$. Thus, the capacity of the

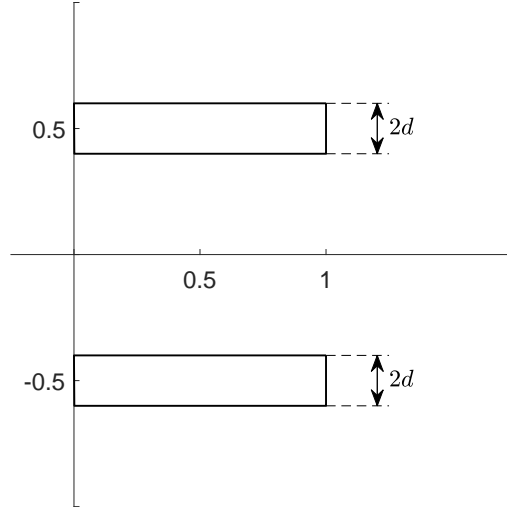


FIGURE 28. The domain G in the exterior of the rectangular closed sets for $d = 0.1$.

TABLE 10. The approximate values of the capacity for the domain exterior to the two rectangles.

d	Capacity	Time (sec)
0.4	7.55672805385065	2.1
0.3	4.55284511607753	2.1
0.2	3.3856923786737	2.0
0.1	2.68688786213937	2.0
0.05	2.40554719800866	2.1
0.02	2.24063059387802	2.4
0.01	2.18262548680027	2.8
0.005	2.15161636330889	4.9
0	2.11577897412447	25.0

domain R_2 equals to the capacity of R_3 which can be expressed by [V2, 5.60 (1)]

$$(8.2) \quad \text{cap}(R_2) = \frac{\pi}{\mu(1/\sqrt{1+s})}, \quad s = \frac{4k}{(1-k)^2}.$$

Here μ is the function defined in (3.7).

By [BF, 119.03], the domain R_2 can be mapped conformally also onto the unbounded doubly connected domain R_4 in the exterior of the two slits $[-t/2 - ib/2, -t/2 + ib/2]$ and $[t/2 - ib/2, t/2 + ib/2]$ with

$$t = \frac{2}{k} (E(k) - (1 - k^2 a^2)K(k)), \quad b = \frac{2}{k} (E(k'_1, k') - k^2 a^2 F(k'_1, k'))$$



FIGURE 29. The domain G in the exterior of a vertical rectangular closed set in the upper half-plane (left) and its image \hat{G} under the auxiliary map Ψ (right) for $d = 0.1$.

where the functions $E(k)$, $K(k)$ are defined in (3.6) and (3.5), resp., and

$$F(z, k) = \int_0^z \frac{dw}{\sqrt{(1-w^2)(1-k^2w^2)}}, \quad E(z, k) = \int_0^z \sqrt{\frac{1-k^2w^2}{1-w^2}} dw,$$

and

$$k' = \sqrt{1-k^2}, \quad a = \frac{E(k')}{k^2 K(k')}, \quad k_1 = \frac{k}{k'} \sqrt{a^2 - 1}, \quad k'_1 = \sqrt{1-k_1^2}.$$

Hence $\text{cap}(R_4) = \text{cap}(R_2)$. Further, it is clear that the domain R_1 can be conformally mapped by the function $\hat{\Psi}(z) = i(z - 1/2)$ onto the domain R_4 if we choose k such that $t = b = 1$. Thus, the exact value of the capacity of R_1 is given by

$$(8.3) \quad \text{cap}(R_1) = \frac{\pi}{\mu(1/\sqrt{1+s})}, \quad s = \frac{4k}{(1-k)^2}$$

where k satisfies the equations

$$(8.4) \quad 1 = \frac{2}{k} (E(k) - (1 - k^2 a^2) K(k)), \quad 1 = \frac{2}{k} (E(k'_1, k') - k^2 a^2 F(k'_1, k')).$$

The equations (8.4) are solved using Mathematica for k and the value of the capacity of R_1 computed through (8.3) is 2.1157789709245134. This value agrees with the value presented at the bottom of Table 10 with relative error 1.5×10^{-9} .

8.5. A vertical rectangle in the upper half-plane. Consider the doubly connected domain G in the exterior of the rectangular closed set

$$[0.5 - d, 0.5 + d] \times [1, 2]$$

in the upper half-plane where $0 < d < 0.5$ (see the Figure 29 for $d = 0.1$).

The the auxiliary map

$$(8.6) \quad w = \Psi(z) = \frac{iz + 1}{z + i}$$

TABLE 11. The approximate values of the capacity for the domain exterior to a vertical rectangle in the upper half-plane.

d	$\text{cap}(G)$	Time (sec)
0.4	3.71752232703208	2.4
0.3	3.46693660197964	2.2
0.2	3.20488821317939	2.2
0.1	2.9209225535743	2.3
0.05	2.76128813737089	2.6
0.02	2.65173985860514	3.0
0.01	2.60986001541974	3.9
0.005	2.58658944233183	5.4
0	2.55852314234082	16.4

is used to transform the domain G onto a domain \hat{G} interior to the unit disk and exterior to the piecewise smooth Jordan curve L which is the image of the rectangle under the map Ψ . Then G and \hat{G} have the same capacities. We use the function `annq` with $n = 2^{15}$ to compute the capacity of \hat{G} for several values of d . When $d = 0$, the rectangle reduced to the slit $[i, 2i]$. For the upper half-plane with the slit $[i, 2i]$, we can use the numerical method presented in Section 6 to compute the capacity of the domain exterior to this slit in the upper half-plane. The results are presented in Table 11. The exact value of the capacity of the domain exterior to slit $[i, 2i]$ in the upper half-plane can be computed from (6.1) and is equal to $2\pi/\mu(1/3) = 2.55852314234201$. This exact value agrees with the result presented at the bottom of Table 11 with relative error 4.7×10^{-13} .

8.7. A horizontal rectangle in the upper half-plane. Consider the doubly connected domain G in the exterior of the rectangular closed set

$$[0, 1] \times [0.5 - d, 0.5 + d]$$

in the upper half-plane where $0 < d < 0.5$ (see the Figure 30). By symmetry, the capacity for this domain is 2 times the capacity for the two rectangles case considered in Subsection 8.1.

As in the previous example, the the auxiliary map $w = \Psi(z)$ in (8.6) is used to transform the domain G onto a domain \hat{G} interior to the unit disk and exterior to a piecewise smooth Jordan curve (see Figure 30). Then G and \hat{G} have the same capacities. We use the function `annq` with $n = 2^{15}$ to compute the capacity of \hat{G} for several values of d .

When $d = 0$, the rectangle reduced to the slit $[0.5i, 1 + 0.5i]$. By symmetry, the capacity for the half-plane with the horizontal slit $[0.5i, 1 + 0.5i]$ is 2 times the capacity for the cases of the domain exterior to the two horizontal slits $[i/2, 1 + i/2]$ and $[-i/2, 1 - i/2]$ considered in Subsection 8.1. Thus, according to the exact capacity presented in Subsection 8.1, the exact capacity for the upper half-plane with the horizontal slit $[0.5i, 1 + 0.5i]$ is 4.23155794184903.

For numerical computing of the capacity of the upper half-plane with the slit $[0.5i, 1 + 0.i]$, we use the method presented in Section 6. The obtained result is presented at the bottom



FIGURE 30. The domain G in the exterior of a horizontal rectangular closed set in the upper half-plane (left) and its image \hat{G} under the auxiliary map Ψ (right) for $d = 0.1$.

TABLE 12. The approximate values of the capacity for the domain exterior to a horizontal rectangle in the upper half-plane.

d	$\text{cap}(G)$	$\text{cap}(G)/2$	Time (sec)
0.4	15.1134561077006	7.5567280538503	2.6
0.3	9.10569023215289	4.55284511607644	2.5
0.2	6.77138475734822	3.38569237867411	2.3
0.1	5.37377572427995	2.68688786213998	2.4
0.05	4.81109439601605	2.40554719800803	2.5
0.02	4.48126118775531	2.24063059387766	3.1
0.01	4.36525097360269	2.18262548680134	4.1
0.005	4.30323272661648	2.15161636330824	5.7
0	4.2315579463472	2.1157789731736	23.0

of Table 12. The computed approximate value agrees with the exact value with relative error 1.1×10^{-9} .

Finally, the third column in Table 12 shows halves of the computed values of the capacity for the domain presented in this section. The values presented in the third column agrees with the results presented in Table 10 for two rectangle case.

8.8. A rectangle in a strip. Consider the doubly connected domain G in the exterior of the rectangular closed set

$$[0, 1] \times [-d, d]$$

in the infinite strip $|\text{Im } z| < \frac{\pi}{2}$ where $0 < d < 0.5$ (see the Figure 31).

The the auxiliary map

$$w = \Psi(z) = \tanh \frac{z}{2}$$

is used to transform the domain G onto a domain \hat{G} interior to the unit disk and exterior to the piecewise smooth Jordan curve L which is the image of the rectangle under the

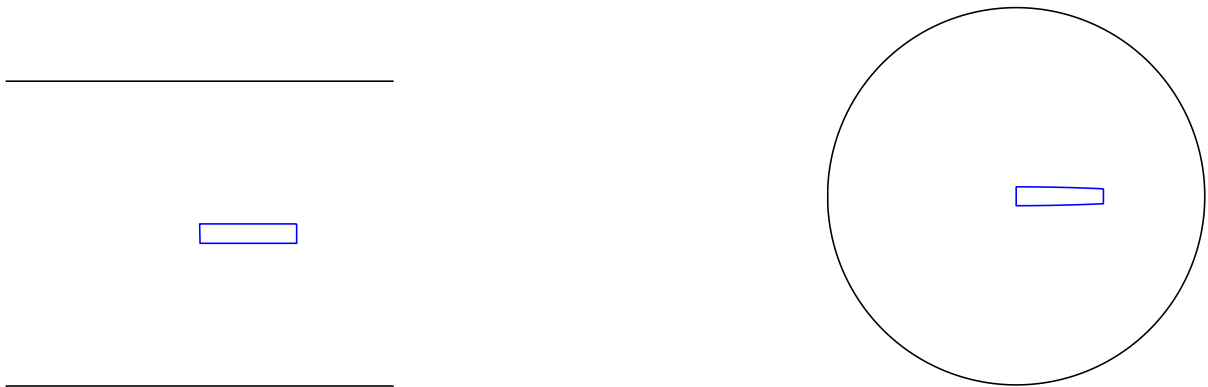


FIGURE 31. The domain G in the exterior of a rectangular closed set in the infinite strip $|\operatorname{Im} z| < \frac{\pi}{2}$ (left) and its image \hat{G} under the auxiliary map Φ (right) for $d = 0.1$.

TABLE 13. The approximate values of the capacity for the domain exterior to a rectangle in the infinite strip $|\operatorname{Im} z| < \frac{\pi}{2}$.

d	$\operatorname{cap}(G)$	Time (sec)
0.4	4.70195555995059	2.3
0.3	4.2845825515985	2.2
0.2	3.88309284384213	2.2
0.1	3.47764983048934	2.3
0.05	3.26000542303295	2.3
0.02	3.11421869705859	2.9
0.01	3.05924909118391	3.5
0.005	3.02891993792618	4.9
0	2.99266869365734	14.1

map Ψ . Then G and \hat{G} have the same capacities. We use the function `annq` with $n = 2^{15}$ to compute the capacity of \hat{G} for several values of d . When $d = 0$, the rectangle reduced to the slit $[0, 1]$. The capacity of the domain exterior to this slit in the strip $|\operatorname{Im} z| < \frac{\pi}{2}$ is computed using the numerical method presented in Section 7. The obtained numerical results are presented in Table 13.

For the domain exterior to slit $[0, 1]$ in the strip $|\operatorname{Im} z| < \frac{\pi}{2}$, the exact value of the capacity can be computed from (7.8) and is equal to $2\pi/\mu(\tanh(1/2)) = 2.99266869365819$. This exact value agrees with the result presented at the bottom of Table 11 with relative error 2.8×10^{-13} .

9. THE HYPERBOLIC CAPACITY AND THE ELLIPTIC CAPACITY

Let E be a compact and connected set (not a single point) in the unit disk \mathbb{D} . In this section, we use the MATLAB function `annq` in Subsection 2.23 to compute the hyperbolic

capacity and the elliptic capacity of the set E . Both the hyperbolic capacity and the elliptic capacity are invariants under conformal mappings

9.1. The hyperbolic capacity The hyperbolic capacity of E , $\text{caph}(E)$, is defined by [Va, p. 19]

$$(9.2) \quad \text{caph}(E) = \lim_{n \rightarrow \infty} \left[\max_{z_1, \dots, z_n \in E} \prod_{1 \leq k < j \leq n} \left| \frac{z_k - z_j}{1 - z_k \bar{z}_j} \right| \right]^{\frac{2}{n(n-1)}}.$$

For the hyperbolic capacity, we assume G is the bounded doubly connected domain defined by $G = \mathbb{D} \setminus E$ such that G can be mapped conformally onto an annulus $q < |w| < 1$. Hence the hyperbolic capacity $\text{caph}(E)$ is given by [DK]

$$(9.3) \quad \text{caph}(E) = q.$$

The constant q can be computed by the function `annq`.

9.4. The elliptic capacity For the compact and connected set E , we define the antipodal set $E^* = \{-1/\bar{a} : a \in E\}$. Since we assume $E \subset \mathbb{D}$, we have $E \cap E^* = \emptyset$ (in this case, the set E is called “elliptically schlicht” [DK]). The elliptic capacity of E , $\text{cape}(E)$, is defined by [DK]

$$(9.5) \quad \text{cape}(E) = \lim_{n \rightarrow \infty} \left[\max_{z_1, \dots, z_n \in E} \prod_{1 \leq k < j \leq n} \left| \frac{z_k - z_j}{1 + z_k \bar{z}_j} \right| \right]^{\frac{2}{n(n-1)}}.$$

To compute the elliptic capacity, we assume G is the doubly connected domain between E and E^* such that G can be mapped conformally onto an annulus $r < |w| < 1/r$. Then the elliptic capacity is given by [DK]

$$\text{cape}(E) = r.$$

Here, the domain G could be bounded or unbounded. We shall use the method presented in Section 2 to map the domain G onto an annulus $q < |w| < 1$ which is conformally equivalent to the annulus $r < |w| < 1/r$ with $r = \sqrt{q}$. Thus, we have

$$(9.6) \quad \text{cape}(E) = \sqrt{q}.$$

We compute q using the function `annq`.

Finally, as our interest in this paper is only in closed and connected subset E of the unit disk \mathbb{D} and comparing numerically between the values of $\text{cape}(E)$ and $\text{caph}(E)$, it is worth mentioning that Duren and Kühnau [DK] have proved that

$$\text{cape}(E) \leq \text{caph}(E),$$

with equality if and only if $E = -E$. This inequality is verified numerically in the following numerical examples.

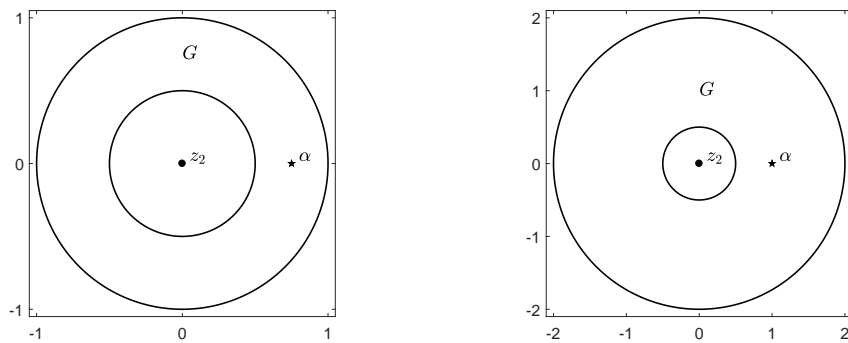


FIGURE 32. The domain G for computing the hyperbolic capacity (left) and the elliptic capacity (right) of $E = \{z \in \mathbb{C} : |z| \leq r\}$ for $r = 0.5$.

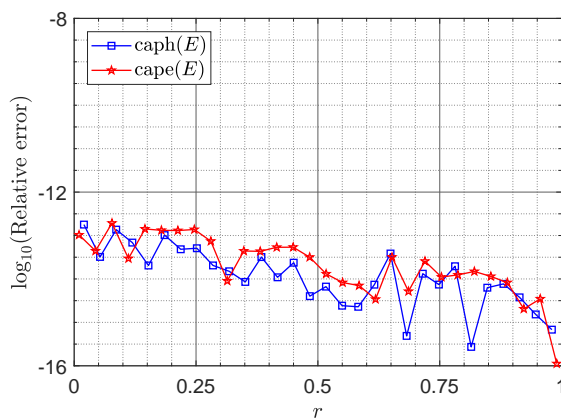


FIGURE 33. The relative error in the computed capacities $c(E)$, $\text{caph}(E)$, and $\text{cape}(E)$ for the disk $E = \{z \in \mathbb{C} : |z| \leq r\}$.

9.7. A disk. As our first example, we compute the hyperbolic capacity and the elliptic capacity of the disk $E = \{z \in \mathbb{C} : |z| \leq r\}$, $0 < r < 1$. For this set E , both capacities are equal where [Ki, DK]

$$\text{caph}(E) = \text{cape}(E) = r.$$

For computing $\text{caph}(E)$, we use the function `annq` with $\alpha = (1+r)/2$ and $z_2 = 0$ to compute the value of q for the conformal map of the doubly connected domain $G = \mathbb{D} \setminus E$ (see Figure 32 (left)) onto the annulus $q < |w| < 1$ and hence $\text{caph}(E) = q$. For $\text{cape}(E)$, the domain G between E and E^* is the bounded doubly connected domain $r < |z| < 1/r$ (see Figure 32 (right)). We use the MATLAB function `annq` with $\alpha = 1$ and $z_2 = 0$ to compute the value of q for the conformal map of this domain G onto the annulus $q < |w| < 1$ and hence $\text{cape}(E) = \sqrt{q}$. For both cases, we use $n = 2^{12}$ and $0.02 \leq r \leq 0.98$. The relative error in the obtained results for $\text{caph}(E)$ and $\text{cape}(E)$ are shown in Figure 33.

9.8. A square. For the second example, we assume E is the closed set $[-r, r] \times [-r, r]$, $0 < r < 1/\sqrt{2}$. For computing $\text{caph}(E)$, the domain G is the bounded doubly connected domain in the interior of the unit circle and in the exterior of the square (see Figure 34

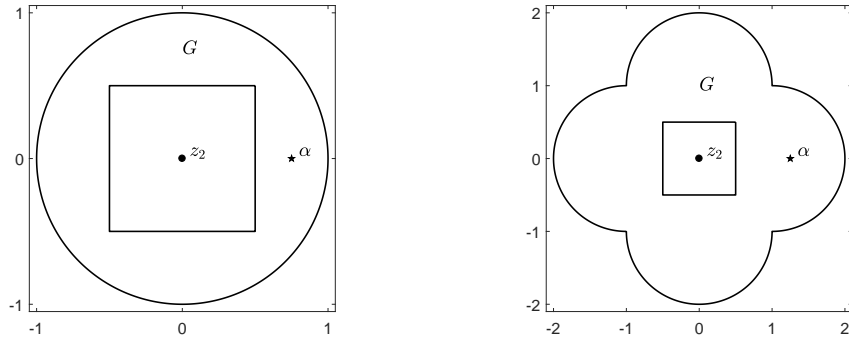


FIGURE 34. The domain G for computing the hyperbolic capacity (left) and the elliptic capacity (right) of $E = [-r, r] \times [-r, r]$ for $r = 0.5$.

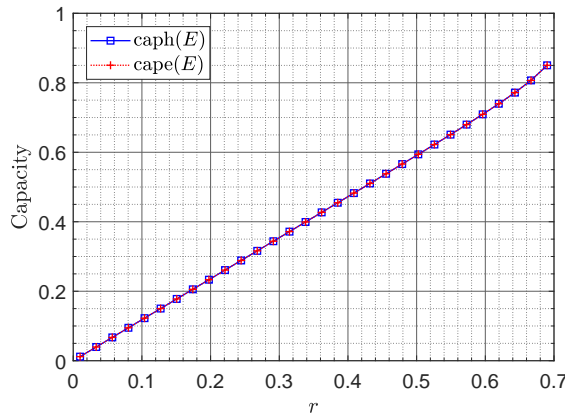


FIGURE 35. The capacities $\text{caph}(E)$ and $\text{cape}(E)$ for $E = [-r, r] \times [-r, r]$.

(left)). We use the function `annq` with $\alpha = (1+r)/2$ and $z_2 = 0$ to compute q and then $\text{caph}(E) = q$. For $\text{cape}(E)$, the domain G is the bounded doubly connected domain between E and E^* (see Figure 34 (right)). Hence, $\text{cape}(E) = \sqrt{q}$ where q is computed using the function `annq` with $\alpha = (r + 1/r)/2$ and $z_2 = 0$. For both cases, we use $n = 2^{13}$ for $0.02 \leq r \leq 0.69$. The obtained results are shown in Figure 35. This set E is symmetric where $E = -E$, and hence $\text{caph}(E) = \text{cape}(E)$.

9.9. Amoeba-shaped boundary. For the third example, we compute $\text{caph}(E)$ and $\text{cape}(E)$ of E where E is the closed region bordered by the amoeba-shaped boundary L with the parametrization

$$\eta(t) = 0.1 + 0.6i + 0.2 (e^{\cos t} \cos^2 2t + e^{\sin t} \sin^2 2t) e^{-it}, \quad 0 \leq t \leq 2\pi.$$

For the hyperbolic capacity $\text{caph}(E)$, the domain G is the bounded doubly connected domain in the interior of the unit circle and in the exterior of the curve L (see Figure 36 (left)). Then $\text{caph}(E) = q$ where q is computed using the function `annq` with $\alpha = 0$ and $z_2 = 0.25 + 0.5i$. To compute $\text{cape}(E)$, the domain G is the unbounded doubly connected domain in the exterior of E and E^* (see Figure 36 (right)). We use the function `annq` with

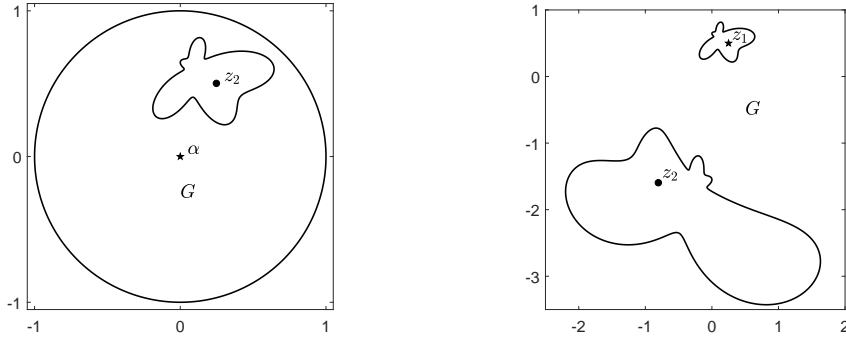


FIGURE 36. The domain G for computing the hyperbolic capacity (left) and the elliptic capacity (right) of the closed region bordered by the amoeba-shaped boundary E .

TABLE 14. The approximate values of the capacities of the closed region bordered by the amoeba-shaped boundary E .

n	$\text{caph}(E)$	$\text{cape}(E)$
64	0.521349946390291	0.25872431985379
128	0.521358819409768	0.258724285703159
256	0.521358832558364	0.258724285703154
512	0.521358832558375	0.258724285703153
1024	0.52135883255838	0.258724285703155
2048	0.521358832558369	0.258724285703154
4096	0.521358832558378	0.258724285703156

$z_1 = 0.25 + 0.5i$ and $z_2 = -1/\bar{z}_1$ to compute the value of q and hence $\text{cape}(E) = \sqrt{q}$. The approximate values of the capacities $\text{caph}(E)$ and $\text{cape}(E)$ for several values of n are shown in Table 14. As the set E is not symmetric, the presented numerical results confirmed the inequality $\text{cape}(E) < \text{caph}(E)$.

9.10. An interval. As our last example, we compute $\text{caph}(E)$ and $\text{cape}(E)$ of the interval $E = [0, r]$, $0 < r < 1$. We first introduce the elementary mappings

$$\Psi_1(z) = \frac{z}{r}, \quad \Psi_2(z) = \frac{1}{4} \left(z + \frac{1}{z} \right) + \frac{1}{2},$$

where the function Ψ_2 maps conformally the exterior of the unit circle onto the exterior of the segment $[0, 1]$. Hence, the inverse function

$$\Psi_2^{-1}(z) = (2z - 1) \left(1 + \sqrt{1 - \frac{1}{(2z - 1)^2}} \right),$$

maps the segment $[0, 1]$ onto the unit circle and the exterior of the segment $[0, 1]$ onto the exterior of the unit circle, where we choose the branch for which $\sqrt{1} = 1$.

The exact value of the hyperbolic capacity of E is [Ki]

$$\text{caph}(E) = e^{-\mu(r)}.$$

For computing $\text{caph}(E)$ numerically, the domain G is the domain exterior of the segment $[0, r]$ and interior to the unit circle $|z| = 1$. We use the mapping function $\zeta = (\Psi_2^{-1} \circ \Psi_1)(z)$ to conformally map the domain G onto the domain \hat{G} exterior to the unit circle $|\zeta| = 1$ and interior to a smooth Jordan curve which is the image of the unit circle $|z| = 1$ under the mapping function $\Psi_2^{-1} \circ \Psi_1$. Then, we use the function `annq` with $\alpha = \Phi_2^{-1}(\Phi_1(0.5i))$ and $z_2 = 0$ to compute the value of q for the conformal map of this domain \hat{G} onto the annulus $q < |w| < 1$ and hence, by (9.3), $\text{caph}(E) = q$.

For the elliptic capacity $\text{cape}(E)$, the domain G is the domain exterior to the finite segment $E = [0, r]$ and the infinite segments $E^* = [-\infty, -1/r]$. The mapping function $(\Psi_2^{-1} \circ \Psi_1)(z)$ maps the domain G onto the domain G_1 exterior to the unit circle and the infinite segment $[-\infty, -(2 + r^2 + 2\sqrt{1 + r^2})/r^2]$. Then, the function

$$\Psi_3(z) = \frac{-1}{z},$$

maps the unbounded domain G_1 onto the bounded domain G_2 interior to the unit circle and exterior to the segment $[0, \tau]$ where

$$\tau = \frac{-1}{-(2 + r^2 + 2\sqrt{1 + r^2})/r^2} = \frac{r^2}{2 + r^2 + 2\sqrt{1 + r^2}}.$$

Thus $\text{cap}(G_2) = \frac{2\pi}{\mu(\tau)}$ (see [LV]). In view of (2.24), it follows from (2.2) that G_2 is conformally equivalent to the annulus $q < |w| < 1$ with $q = e^{-\mu(\tau)}$. Hence, by (9.6), the exact value of the elliptic capacity of E is

$$\text{cape}(E) = e^{-\mu(\tau)/2}.$$

To use the presented method to compute the elliptic capacity $\text{cape}(E)$ numerically, we use the mapping function

$$\zeta = \Psi_4(z) = \frac{z}{\tau},$$

to map the bounded domain G_2 onto the bounded domain G_3 exterior to the segment $[0, 1]$ and interior to the circle $|\zeta| = 1/\tau$. Finally, the function $\xi = \Psi_2^{-1}(\zeta)$ maps the domain G_3 onto the bounded domain \hat{G} exterior to the unit circle and interior to a smooth Jordan curve which is the image of the circle $|\zeta| = 1/\tau$ under the mapping function Ψ_2^{-1} . Thus, the bounded doubly connected domain \hat{G} is the image of the original domain G under the mapping $\Psi_2^{-1} \circ \Psi_4 \circ \Psi_3 \circ \Psi_2^{-1} \circ \Psi_1$. Then, we use the function `annq` with $\alpha = \Phi_2^{-1}(\Phi_4(0.5i))$ and $z_2 = 0$ to compute the value of q for the conformal map from this domain \hat{G} onto the annulus $q < |w| < 1$ and hence, by (9.6), $\text{cape}(E) = \sqrt{q}$.

For both cases, the relative error in the obtained results for $0.02 \leq r \leq 0.98$ is shown in Figure 37 (right). Figure 37 (left) shows also the computed capacities. For both cases, we use $n = 2^{12}$.

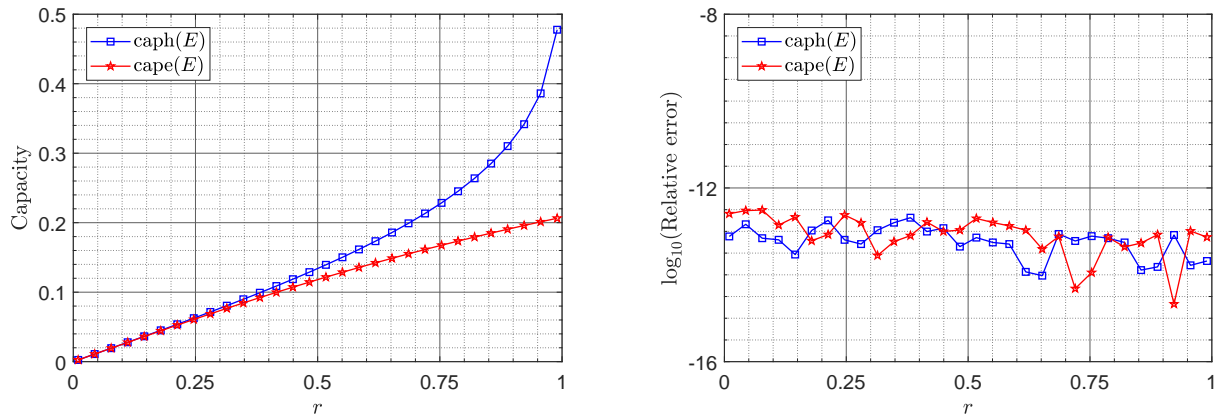


FIGURE 37. The capacities $\text{caph}(E)$ and $\text{cape}(E)$ for the interval $E = [0, r]$ (left), and the relative error in the computed capacities (right).

10. CONCLUDING REMARKS

Conformal invariants are important tools for complex analysis with many applications. However, these invariants can be expressed explicitly only in very few special cases. Thus, numerical methods are required to compute these invariants. A numerical method for computing some conformal invariants is presented in this paper. The method can be used for domains with different types of boundaries including domains with smooth or piecewise smooth boundaries. The performance and the accuracy of the presented method is compared to analytic solutions or to previous results whenever analytic solutions or previous results are available. Further, a MATLAB implementation of the proposed method is given in the MATLAB function `annq` in Subsection 2.23. This MATLAB function was used in almost all examples in this paper to compute the conformal capacity, the hyperbolic capacity and the elliptic capacity. For some examples, an auxiliary procedure is required before using the function `annq`. All the computer codes of our computations are available in the internet link <https://github.com/mmsnasser/cci>.

REFERENCES

- [Ah] L.V. AHLFORS: Conformal invariants. McGraw-Hill, New York, 1973.
- [AKT] A.P. AUSTIN, P. KRAVANJA, AND L.N. TREFETHEN: Numerical algorithms based on analytic function values at roots of unity. *SIAM J. Numer. Anal.* 52 (2014) 1795–1821.
- [AVV] G. D. ANDERSON, M. K. VAMANAMURTHY, AND M. VUORINEN: Conformal invariants, inequalities and quasiconformal maps. J. Wiley, 1997.
- [AST] N. AOYAMA, T. SAKAJO AND H. TANAKA: A computational theory for spiral point vortices in multiply connected domains with slit boundaries. *Japan J. Indust. Appl. Math.* 30 (2013), 485–509.
- [At] K.E. ATKINSON: The Numerical Solution of Integral Equations of the Second Kind. Cambridge University Press, 1997.
- [BSV] D. BETSAKOS, K. SAMUELSSON, AND M. VUORINEN: The computation of capacity of planar condensers. *Publ. Inst. Math. (Beograd) (N.S.)* 75(89) (2004), 233–252.

- [BBG] S. BEZRODNYKH, A. BOGATYREV, S. GOREINOV, O. GRIGORIEV, H. HAKULA, AND M. VUORINEN: On capacity computation for symmetric polygonal condensers. *J. Comput. Appl. Math.* 361 (2019), 271–282.
- [Bo] F. BOWMAN: *Introduction to Elliptic Functions with Applications*, English Universities Press Ltd., London, 1953.
- [BF] P.F. BYRD AND M. D. FRIEDMAN: *Handbook of elliptic integrals for engineers and scientists*. Second edition, revised. Springer-Verlag, Berlin, 1971.
- [DNV] D.DAUTOVA, S.NASYROV AND M.VUORINEN: Conformal module of the exterior of two rectilinear slits. arXiv:1908.02459, (2019).
- [DEK] T.K. DELILLO, A.R. ELCRAT AND E.H. KROPPF: Calculation of resistances for multiply connected domains using Schwarz-Christoffel transformations. *Comput. Methods Funct. Theory* 11 (2011), 725–745.
- [DT] T.A. DRISCOLL AND L.N. TREFETHEN: *Schwarz-Christoffel mapping*. Cambridge University Press, Cambridge, 2002.
- [Du] V. N. DUBININ: *Condenser Capacities and Symmetrization in Geometric Function Theory*, Birkhäuser, 2014.
- [DK] P. DUREN AND R. KÜHNAU: Elliptic capacity and its distortion under conformal mapping. *Journal d’Analyse Mathématique* 89(1) (2003) 317–335.
- [ET] M. EMBREE AND L.N. TREFETHEN: Green’s Functions for Multiply Connected Domains via Conformal Mapping. *SIAM Rev.* 41 (1999), 745–761.
- [GM] J.B. GARNETT AND D.E. MARSHALL: *Harmonic measure*. Reprint of the 2005 original. Cambridge University Press, Cambridge, 2008.
- [GG] L. GREENGARD AND Z. GIMBUTAS: FMMLIB2D: A MATLAB toolbox for fast multipole method in two dimensions. Version 1.2, <http://www.cims.nyu.edu/cmcl/fmm2dlib/fmm2dlib.html>. Accessed 1 Jan 2018.
- [HRV1] H. HAKULA, A. RASILA AND M. VUORINEN: On moduli of rings and quadrilaterals: algorithms and experiments. *SIAM J. Sci. Comput.* 33 (2011), no. 1, 279–302.
- [HRV2] H. HAKULA, A. RASILA AND M. VUORINEN: Computation of exterior moduli of quadrilaterals. *Electron. Trans. Numer. Anal.* 40 (2013), 436–451.
- [HRV3] H. HAKULA, A. RASILA AND M. VUORINEN: Conformal modulus on domains with strong singularities and cusps. *Electron. Trans. Numer. Anal.* 48, (2018), 462–478.
- [KNV] E. KALMOUN, M.M.S NASSER AND M. VUORINEN: Numerical computation of Mityuk’s function and radius for circular/radial slit domains. arXiv:1908.03874, (2019).
- [KL] L. KEEN AND N. LAKIC: *Hyperbolic geometry from a local viewpoint*. Cambridge University Press, Cambridge, 2007.
- [Ki] S. KIRSCH: Transfinite diameter, Chebyshev constant and capacity. In: *Handbook of complex analysis: geometric function theory*. Vol. 2, 243–308, Elsevier Sci. B. V., Amsterdam, 2005.
- [K1] R. KRESS: A Nyström method for boundary integral equations in domains with corners. *Numer. Math.* 58(2) (1990), 145–161.
- [K2] R. KRESS: *Linear Integral Equations*. Springer, New York, 2014.
- [Ku] R. KÜHNAU, ED.: *Handbook of complex analysis: geometric function theory*. Vol. 1, 2002, Vol. 2, 2005, Edited by R. Kühnau. Elsevier Science B.V., Amsterdam, 2005.
- [LV] O. LEHTO AND K.I. VIRTANEN: *Quasiconformal mappings in the plane*, 2nd edition, Springer, Berlin, 1973.
- [LSN] J. LIESEN, O. SÉTE AND M.M.S. NASSER: Fast and accurate computation of the logarithmic capacity of compact sets. *Comput. Methods Funct. Theory* 17 (2017), 689–713.
- [N1] M.M.S. NASSER: Numerical conformal mapping via a boundary integral equation with the generalized Neumann kernel. *SIAM J. Sci. Comput.* 31 (2009), 1695–1715.

- [N2] M.M.S. NASSER: Numerical conformal mapping of multiply connected regions onto the second, third and fourth categories of Koebe's canonical slit domains. *J. Math. Anal. Appl.* 382 (2011), 47–56.
- [N3] M.M.S. NASSER: Fast solution of boundary integral equations with the generalized Neumann kernel. *Electron. Trans. Numer. Anal.* 44 (2015), 189–229.
- [N4] M.M.S. NASSER: Numerical computing of preimage domains for bounded multiply connected slit domains. *J. Sci. Comput.* 78 (2019) 582–606.
- [NF] M.M.S. NASSER AND F.A.A. AL-SHIHRI: A fast boundary integral equation method for conformal mapping of multiply connected regions. *SIAM J. Sci. Comput.* 33 (2013), A1736–A1760.
- [NG] M.M.S. NASSER AND C.C. GREEN: A fast numerical method for ideal fluid flow in domains with multiple stirrers. *Nonlinearity* 31 (2018), 815–837.
- [NMZ] M.M.S. NASSER, A.H.M. MURID AND Z. ZAMZAMIR: A boundary integral method for the Riemann-Hilbert problem in domains with corners. *Complex Var. Elliptic Equ.* 53 (2008), 989–1008.
- [NV] M.M.S. NASSER AND M. VUORINEN: Numerical computation of the capacity of generalized condensers. *arXiv:1908.03866*, (2019).
- [OLBC] F. W. J. OLVER, D. W. LOZIER, R. F. BOISVERT, AND C. W. CLARK, EDs.: *NIST Handbook of Mathematical Functions*, Cambridge Univ. Press 2010, <http://dlmf.nist.gov>
- [PS] N. PAPAMICHAEL AND N. STYLIANOPOULOS: Numerical conformal mapping. Domain decomposition and the mapping of quadrilaterals. World Scientific Publishing Co. Pte. Ltd., Hackensack, NJ, 2010.
- [SL] R. SCHINZINGER AND P. A. A. LAURA: Conformal mapping. Methods and applications. Revised edition of the 1991 original. Dover Publications, Inc., Mineola, NY, 2003.
- [ST] E.B. SAFF AND V. TOTIK: Logarithmic potentials with external fields. Springer-Verlag, Berlin, 1997.
- [TW] L.N. TREFETHEN AND J. A. C. WEIDEMAN: The exponentially convergent trapezoidal rule. *SIAM Review* 56 (2014), 385–458.
- [Va] A. VASIL'EV: Moduli of Families of Curves for Conformal and Quasiconformal Mappings. Springer-Verlag, Berlin, 2002.
- [V1] M. VUORINEN: Conformal invariants and quasiregular mappings. *J. Anal. Math.* 45 (1985), 69–115.
- [V2] M. VUORINEN: Conformal geometry and quasiregular mappings. *Lecture Notes in Mathematics*, 1319. Springer-Verlag, Berlin, 1988.
- [WN] R. WEGMANN AND M.M.S. NASSER: The Riemann-Hilbert problem and the generalized Neumann kernel on multiply connected regions. *J. Comput. Appl. Math.* 214 (2008), 36–57.

E-mail address: `mms.nasser@qu.edu.qa`

E-mail address: `vuorinen@utu.fi`

DEPARTMENT OF MATHEMATICS, STATISTICS AND PHYSICS, QATAR UNIVERSITY, P.O. Box 2713, DOHA, QATAR.

DEPARTMENT OF MATHEMATICS AND STATISTICS, UNIVERSITY OF TURKU, TURKU, FINLAND.